5-2015

Surface characterization of 316L stainless steel for biomedical applications

Lawrence Cano
University of Texas-Pan American

SURFACE CHARACTERIZATION OF 316L STAINLESS STEEL FOR BIOMEDICAL APPLICATIONS

A Thesis

by

LAWRENCE CANO

Submitted to the Graduate School of
The University of Texas-Pan American
In partial fulfillment of the requirements for the degree of

MASTER OF SCIENCE

May 2015

Major Subject: Mechanical Engineering

SURFACE CHARACTERIZATION OF 316L STAINLESS STEEL FOR BIOMEDICAL APPLICATIONS

A Thesis
by
LAWRENCE CANO

COMMITTEE MEMBERS

Dr. Waseem Haider
Chair of Committee

Dr. Karen Lozano
Committee Member

Dr. Jiaznhi Li
Committee Member

May 2015

ABSTRACT

Cano, Lawrence. Surface Characterization of 316 L Stainless Steel for Biomedical Applications. Master of Science (MS), May, 2015, 109 pp. 9 tables, 21 figures, 120 references, 40 titles.

Stainless steel alloys play an important role in the field of biomaterials due to their exceptional corrosion resistance and biocompatibility. These alloys have the capability to enhance the quality of a human life by altering various structures of human physiology. The close proximity these alloys have with destructive body fluids, ion dissolution is a detrimental cause from the corrosion initiative and may cause unfavorable reactions. A view on developing an improved compatible surface for the human body leads to implementation of different chemical surface modifications used for creating features that must be corrosion resistant and biologically active without changing the overall bulk property. In this study, multiple technics for chemical treatments of above and below enhanced oxidation evolution will undergo a process of electropolishing and magnetoelctropolishing produced on commercial 316 L stainless steel. These surface modifications attempt to refine and improve critical features: corrosion resistance, biocompatibility, morphology, wettability, and chemistry.

DEDICATION

The completion of my master studies and this thesis would have not been possible without the love and support from my beloved family. My mother, Rosa Cano, my father Joe Cano, and my sister, Roxanne Cano, enthusiastically inspired and encouraged me by every means necessary to accomplish this degree. Thank you for your love and patience.

ACKNOWLEDGMENTS

I will always be grateful to Dr. Waseem Haider, chair of my thesis committee, for all his mentoring and advice. From research funding, research objectives, and progression, to manuscript editing, he encouraged my to complete this process through his patience and guidance. My thanks go to my thesis committee members: Dr. Karen Lozano, and Dr. Jianhzi Li. Their advice, input, and comments on my thesis helped to ensure the quality of my intellectual work.

I would want to recognize and thank Ryszard Rokicki from Electrobright who helped with specific electrochemical treatments to support my research. I would also like to acknowledge the US Army Research Office (W911NF-14-1-0100) for their support in the use of the XPS system.

TABLE OF CONTENTS

Page

LIST OF TABLES

LIST OF FIGURES

CHAPTER I

INTRODUCTION

Biomaterials

The route of the biomaterials course is heading through an advancement of revolutionary change, as the importance of material science and engineering is the fundamental foundation. The sophistication at which biomaterials have changed the outlook and outcome on innovation and complexity of their functionalities will unite with acceptance in the human body. The intention of these materials is to imitate a form of physicochemical properties of natural materials, as nature may provide the guidance necessary as a footprint in the right direction with simplicity and efficiency. Not only does nature naturally inspire and create the material, itself, but the conception of these materials will produce defense mechanisms in order to fill the voids of dangerous scenarios. Whereas synthetic materials are typically engineered on the scale of millimeters or larger and then machined to have a micrometer or nanometer scale factor, natural materials are constructed on similar small scale by self-assembly, a completely new beginning means of improvement that enables the construction of detailed information, complex structures in a highly reproducible manner with the minimalist energy input [1]. The extensive knowledge gained from this self-assembly method is being used to project biomaterials on a path for the physiology of the human body to work in unison with biological materials.

The term biomaterials stated by D. F. Williams *et. al.* is defined as “a material intended to interface with biological systems to evaluate, treat, augment or replace any tissue, organ or

function of the body" and further defined the term biocompatibility as "the ability of a material to perform with an appropriate host response in a specific application" [2]. In the last few decades, biomaterials have been used in a wide range of medical device implants such that, in the era of the 21st century, it profoundly is the most important advanced technology covered in the area of the medical field. The terminology of what is considered to be a biomaterial in this day and age would have never been considered 50 years ago because it simply did not exist; medical device manufactures for biomaterials, validated regulatory approved processes, understanding of biocompatibility, and credible academic courses on biomaterials were all non-existent. The history of biomaterials can be conveniently organized into four eras: prehistoric, era of the surgeon hero, designed biomaterials/engineered devices, and the era leading toward the new millennia [3].

Materials, whether natural or artificial have been implemented in a multitude of different medical implant devices, artificial organs, rehabilitation devices, and apparatus materials. Metals, ceramics, and polymers have ideally found their manner into essential applications to an extent that many are now the routine armamentarium of the medical profession [4]. The human body has gained the ability of accepting implant devices on a level for opting to transition to use a biomaterial in place of an artificial heart valve, stent in blood vessels, implant for spinal disks, and hip, knee, and shoulder implants as a few examples, displayed in Table 1. A high number of implants related to spinal, knee, hip, and shoulder replacements have excessive load bearing applications along with complex structures that need to be functional under critical conditions. Considering knee, hip, and shoulders joints being comprised of articling cartilage and connective tissue, the interaction between the implants and surrounding tissue needs to be compatible.

Table 1: Biological substitutes [5]**.**

Organ	Examples
Heart	Cardiac pacemaker, artificial heart valve, artificial heart, blood vessels
Lung	Oxygenator machine
Eye	Contact lens, intraocular lens
Ear	Artificial stapes, cochlea implant
Bone	Bone plate, intramedullary rod
Kidney	Catheters, stent, kidney dialysis machine
Bladder	Catheter, stent

The biological substitutes are not only related to the intent of fixing an issue of a problematic area, but to help treat the patient in hopes of further prolonging the span of perfectly functional systems. Table 2 shows the scope of commonly faced issues and some methods that will help improve the dysfunctional situation the body may be experiencing.

Table 2: Methods of improvement [5]**.**

Issues	Examples
Replacement of diseased or damaged part	Artificial hip joint, kidney dialysis machine
Assist in healing	Sutures, bone plates, screws
Improve function	Cardiac pacemaker, intraocular lens
Correct functional abnormality	Cardiac pacemaker
Correct cosmetic problem	Augmentation mammoplasty
Aid to diagnosis	Probes, catheters
Aid to treatment	Catheters, drains

The selection to use biomaterials has been restricted by this biocompatibility property of the material to meet specific requirements for human analog application and interaction. The biocompatibility can be subjected to different subsets as the human body determines whether or not to accept the implant material or device and have the inclination to generate a positive response. As many of these biomaterials have an important status in modern technology to help replace or treat the physiological anatomy of the bodily systems, efficient innovative new materials with improved performance are sought after with great interest.

History of Biomaterials

As mentioned before, the relative name of biomaterials was not officially introduced as a field until the 1960's, but the concepts this field holds have been implemented for years prior and dates back centuries. The complexity of ancient and primitive methods combined with the simplicity of what nature has provided will complete a learning curve in understanding the first ideologies of concepts that were considered constructive ingenuity.

Sutures, commonly known as stitches, have been used as a medical device to situate body tissue ranging in severity from extensive surgery to the everyday laceration since the Neolithic period. A suture is a thread of material used for wound closure; the ancient Egyptians used linens and Europeans have used fibers from animal intestine to obtain the necessary structural suture material available during that time period. In a rather particularly strange occurrence in finding a viable material, a method of using a natural resource of biting ants to join tissue together in South Africa and India was unusual with a sense of effectiveness. The readily available materials in these periods were influenced by mechanical properties for proper wound closure, as strength is an essential aspect for the material's characteristic. Currently, typical surgical sutures already in clinical use today have been equated with a biocompatible polymer capable of being absorbed, degraded, or remain intact without any complications. The foundation of this system begins with underlying suture being a polymeric material known as polyglycolic acid (PGA) and is widely used throughout the medical field as a common suture.

Dental implants have a broad variety of materials used throughout time ranging from gold, iron, blue nacre shell, ceramics, etc. The Mayan's creativity fashioned an innovative and ingenious way to replace teeth with this blue nacre shell; this hard, durable material was positioned where it would integrate with the jawbone due to the chemistry and architectural

structure. In later years, the Romans and Incas used gold in their own method to improve dental implants.

In 1829 an Alabama doctor, Dr. Henry Levert, began to experiment with the possibility of using metal implants safely in the human body. After testing a multitude of different metals, his overall conclusion found that platinum was better suited to be tolerated rather than gold, silver or lead due to the overall properties. Considering the dangerously toxic effects of lead toward the body, the choice of choosing these metals was positive for long run applications of future development. Surgeons became intrigued over the upcoming decades to possibly use these metals in screws and plates to fixate bones in replace of the less effective method of trusting in splints or braces. In 1886, a German surgeon, H. Hansmann was the first doctor to successfully use these fixation techniques to heal human bone. A break through in 1926, led the way for metals as not much was known with empirical data and very little known about the safety metals impose in the human body. Dr. Arthur Zierold of Minneapolis continued the work of Dr. Levert with astounding findings that resulted in the conclusion that iron and steel corroded promptly in the human body, copper, aluminum, and zinc discolored the surrounding tissue, and gold, aluminum, and silver were not ideal for body fixations. Experiments conducted with a specific type of stainless steel proved to be promising as the alloy allowed for the metal to be used in the body regularly with fewer complications. As time would proceed further, titanium was introduced with even more promising results.

The theories of early philosophers and physicians paved a path for scientists to understand the ideas of the functionality of the cardiovascular system. In 1881, a French scientist named Etienne Jules Marcy came up with a conventional idea and published his design for an artificial human heart. However, it would not be until 100 years later that a similar design would

actually be implemented. In 1982, the first artificial heart was successfully implanted in a human, yielding a life span of 112 days after the implantation surgery. While not long by today's standards, this was much longer than that of what was attempted in previous years. For instance, the results from Dr. Willem Kolff during the late 1950's produced an artificial heart that was implanted into a canine, but only had a life span after the surgery of 90 minutes. Two surgeons named Domingo Liotta and Denton Cooley twelve years later implanted an artificial heart as a secondary measure to prolong the life of a man until a donor heart was available as his life span was only 64 hours after the surgery. As one of Dr. Kloff's graduate students, Robert Jarvik, later developed the "Jarvik-7"; his own design became the first artificial heart permanently implanted in the human body.

After World War II, huge advances in biomaterials were attributed to two factors for the different techniques in using these new materials. Surgeons were given carte blanche, freedom to act as one wishes or thinks is best, in order to save their patients with the limited supplies at hand in the battlefield and many of these surgeons became very creative. Another factor was the availability of plastics "polymers". Over time, physicians began to connect the useful thinking of battlefield surgeons and linked their ideas to practical use of why plastics would be a good material. Plastics can be made to be light, inert, biodegradable, and easy to manufacture into various shapes as opposed to their metal counterpart. An ophthalmologist, Sir Harold Ridley, discovered the possibility of using plastic to create an intraocular lens to treat cataracts from examining the shards imbedded in a fighter pilot's eyes after World War II and noticed no indication of inflammation or irritation. The invention of this lens revolutionized the optics pertaining to the blind. Thus, leading to the first intraocular implant procedure in 1949. In 1952, surgeon Arthur Voorhees had a radical idea to use left over parachute material from the war in

order to create the first-ever synthetic blood vessel. In today's arterial replacement programs, the material typically used is Gore-Tex. It was a vascular surgeon that suggested to the founder and creator of Gore-Tex, Bill Gore, that his material would be ideal for use as a viable artificial blood vessel.

The first attempt at surgery for hip replacement in 1891 was less than that of successful, similar to the attempts made from the 1920's through 1950's. This form of implant or replacement was another idea that did take some time to propagate forward to fully become reality. However, the materials and procedure were perfected in 1961 by surgeon John Charnley from England; his method consisted of a slippery solid, fluid, to lesson the friction in the joint. Between 1960 and 1980 biomaterials as a specific field of study grew increasingly popular. This new concept was a collaboration of different scientists from multiple disciplines: mechanical engineers, electrical engineers, chemical engineers, chemists, and biologists with the same understanding to help advance the new methods of medicine. A leap forward yielding pacemakers, knee replacements, kidney dialysis, breast implants, stents, heart valve replacements as new materials were created such as silicone, Teflon, bio-glass and hydrogels with the same purpose to apply new models to medicine.

The steps to follow were an almost impossible idea to be taken from theoretical application and implement with the same ideas in the laboratories. The next step that the biomaterials path undertook was the creation of actual biological materials. Scientists experimented with being able to grow cartilage and skin from 1970 through 1980 until the tissue-engineering field formed in 1997 when anesthesiologist Charles Vacanti grew a human ear on the adverse rearing of a mouse. The acceleration of the growing different tissues resulted in being able to clone a sheep. Headlines in 2006 from surgeon Anthony Atala and his team from

the Wake Forrest Institute for Regenerative Medicine formally made an announcement that they successfully grew bladders from the patient's own cells and were able to implant these lab-cultivated organs. This was achieved by removing a small piece of tissue from the patient and then growing the cells on a scaffold which typically can take up to eight weeks to cultivate. "This is one small step in our ability to go forward in replacing damaged tissues and organs", quoted by Atala. Fast forwarding to the year 2013, the practice of tissue engineering and experiments continue to lead promising results in being able to effectively culture a miniature human brain with distinct regions after a 20 to 30 day growth period.

Future Development

The future is to rethink about how inspiration is drawn from natural biological specimens and to apply these empirical design principles to new areas. This will lead the biomaterials advancement to develop more functional medical materials and the extent at which biomaterials are brought into new fields of practical application. However, the future may also present an opportunity for practitioners in the field to rethink fundamentally the way in which inspiration is drawn from biology [6]. Understanding the way in which complex dynamic behaviors are accomplished in nature may lead to the design of novel materials that mimic nature not through presenting active patterns replicated exactly from biological molecules but rather through reproducing the functional behavior of these biological materials to obtain properties that are currently unavailable [6]. In the area of research, biomaterials will be constructed of smart, multifunctional nanotechnology as a new generation of implants will be used in the human body. The behaviors of these complex biomaterials are controlled by a combination of various inputs from chemical and physical stimuli. The purpose of these materials is to focus on anatomical regions, monitor health, and mediate biological crises. Biological systems have already inspired

the development of cell-programming matrices based on our abstract understanding of dynamic biological processes such as infection, and these matrices accomplish their task with a small subset of key molecular stimuli [7]. Biosensors capable of interacting with specific cell populations used in diagnostic or therapeutic application are used to generate a cell programming matrix by harnessing the dynamic indictors provided by specific cell types to modify complex devices from basic input templates that are being contemplated to predict diseases.

A critical intellectual step in biomaterials design is the recognition that both biological polymers and organisms can be used as models of, or templates for, multifunctional, dynamic devices and that components of natural systems can be used for purposes other than that which they serve in nature [8]. This understanding is being applied in the context of self-assembling natural materials such as DNA, which originally was considered solely as an information storage system but recently has inspired the development of new types of nanomaterial with precisely defined structures, as well as self-assembling synthetic polymers (inspired by the highly regulated base-pairing of DNA) [9]. Aside from the devices and materials, the future allurement of biological inspiration from nature is to rethink the method or manufacturing to transform raw materials in the chemical and materials industries.

Accomplishing this transformation in the biomaterials field will require an improved understanding of how cells receive information from materials and how key signaling pathways process this information to dictate biological responses; it will not be sufficient enough to simply make materials and empirically test for their effects on cell or host responses [10].

Requirements and Characteristics

Biomaterials with an inert ability toward the physiological environment need to be understood and measured. Without a specific definition to accurately gauge the biocompatibility

of a material, the concept is grasped from the material's performance of the success rate at which its interaction corresponds with its environment. The biocompatibility may be defined particularly for multiple applications including soft tissue, hard tissue, cardiovascular system, etc. for the purpose that would be served in each category. The applications for each category will exemplify the importance of the necessity to fully understand the capability that the material will impose on the body to determine the acceptance or denial in cases relative to the task at hand. As the biocompatibility relates to the other important functions such as toxicity, tissue structure, performance requirements, pathobiology, healing, inflammation, and mechanical requirements, all have an impact on the physiological environment response. The normal requirements for a biomaterial should be non-toxic, except for exclusive scenarios that would require the material to be toxic (i.e. drug delivery systems targeting cancer cells). Unless under one of these unique conditions, non-toxic materials been have developed into a complex science to understand their role in what we would consider a biomaterial. Cell toxicity is a key factor that forces the leaching of ions to be released from the material, causing damaging effects to its surrounding environment. As the ideal situation would be to not release any of these ions from its mass unless specified by an engineered design, the governing rule for the realization of a biomaterial should strictly be considered non-toxic. These methods to evaluate toxicity are always under constant scrutiny on the development of how new biomaterials meet specific criteria.

The healing process of injured or damaged tissue when a device is implanted in the body will generate an inflammatory response surrounding the area and will initiate the beginning of the healing process. A response to some form of foreign substance will cause a reaction that is produced when the foreign material, an implant or device, is in immediate proximity to the

wound location, as this is the normal response of the body to defend against the modification instigated from the implant. Depending on the area or site involved with the biomaterial, reactions will vary in intensity and duration. The understanding of the normal inflammatory response and the alteration of that response due to the foreign body are always under constant inquiry.

The mass of the biomaterial is subjected to a form of mechanical functionalities that are gained from their physical properties. Determining whether the biomaterial will have the mechanical performance, mechanical durability, and physical properties will be based on these functionalities working in cohesion with the human body. The mechanical capabilities of the device are held up to varies constructive designs depending on the location where the device is implemented: strong and rigid, strong and flexible, flexible and tough, or soft and elastomeric. Aside from these characteristics that the material may hold, the function of these structures are not relevant if the durability of the biomaterial is vulnerable to fragile points in designing of the device. The durability of the biomaterial is constructed on the longevity that the device will need to perform and can range from days and months to years. The durability is more than a time period; it is having the biomaterial able to sustain its physical properties the entire duration. These properties are all supported by the mass or bulk of the comprised biomaterial and in order to meet these functions we need to consider the chemistry, mechanical engineering, chemical engineering, biology, physics, and material sciences as one whole entity.

Classification of Biomaterials

A material's effectiveness within the human body may be categorized in multiple ways such as biomaterials being used as devices to substitute an anatomical system in a safe, economic, and physiological approach. Currently in practice is an assortment of devices for

clinical use and the biomaterials used in treatment for disease and or injury range from synthetic to biodegradable materials as part of replacing a living system or the near proximity interaction with living tissue. The Clemson University Advisory Board for Biomaterials has formally defined a biomaterial to be "a systemically and pharmacologically inert substance designed for implantation within or incorporation with living systems" [11]. Additional definitions mention "materials of synthetic as well as of natural origin in contact with tissue, blood, and biological fluids, and intended for use for prosthetic, diagnostic, therapeutic, and storage applications without adversely affecting the living organism and its components" [12] and "any substance (other than drugs) or combination of substances, synthetic or natural in origin, which can be used for any period of time, as a whole or as a part of a system which treats, augments, or replaces any tissue, organ, or function of the body" [13]. According to these definitions one must possess knowledge in a number of different disciplines or collaborate with individuals from a wide variety of different specialties in order to properly develop and use biomaterials in medicine and provide some examples of the uses of biomaterials, which include replacement of a body part that has lost function due to disease or trauma, to assist in healing, to improve performance, and to correct abnormalities [5]. The impact on biotechnology and science has been influenced from the important roles in advancement of countless biomaterials. Table 3 shows a few of the body systems proficient enough to execute the use of a biomaterial.

Table 3: System replacements [5]**.**

System	Examples
Skeleton	Bone plate, joint replacement
Muscular	Sutures, muscle simulator
Nervous	Hydrocephalus drain, cardiac pacemaker, nerve simulator
Endocrine	Microencapsulated pancreatic islet cells
Reproductive	Augmentation mammoplasty, cosmetic replacements

Ceramic Biomaterials

There are a few preferences in the properties of some materials with characteristics unique to itself that dictate important features: non-toxic, non-allergic, non-inflammatory, biocompatible, and bio-functional. Ceramics, in this case, offer these sets of characteristics with relatively hard surfaces, bio-inert, low surface reaction, and biodegradability. Ceramics used in manufactured implants can be classified as non-absorbable or a relatively inert biomaterial, bioactive or surface reactive as a semi-inert biomaterial [14], and being biodegradable considered to be non-inert [15]. Bio-ceramics created from oxides: alumina, zirconia, silicone nitrides, and carbons are inert in the body. Specific glass ceramics and dense hydroxyapatites are semi-inert, bio-reactive, while calcium phosphates and calcium aluminates are absorbable ceramics [16].

Polymer Biomaterials

As opposed to metal or ceramic materials, polymers have an advantage toward the usage as a biomaterial for its simplicity of manufacturing to produce numerous shapes ranging from films, sheets, fibers, etc. These synthetic polymers have been widely used in clinical application for prosthetic materials, dental materials, implants, drug delivery systems, and tissue engineering. The possibilities of polymers being met with the desired mechanical and physical properties are shown in Table 4 while the necessity along with the ease of processing under a reasonable cost will be considered for production value.

Table 4: Polymeric materials [5]**.**

Synthetic Polymers	Examples
Polyvinylchloride	Blood and solution bag, surgical packing, IV sets, dialysis devices, catheter bottles, connects, cannulae
Polyethylene	Pharmaceutical bottle, nonwoven fabric, catheter, pouch, flexible container, orthopedic implants
Polypropylene	Disposable syringes, blood oxygenator membrane, suture, nonwoven fabric, artificial vascular grafts
Polymethylmetacrylate	Blood pump and reservoirs, membrane for blood dialyzer, implantable ocular lens, bone cement
Polystyrene	Tissue culture flasks, roller bottles, filterwares
Polyethylenterephthalate	Implantable suture, mesh, artificial vascular grafts, heart valve
Polytetrafluoroethylene	Catheter, artificial vascular grafts
Polyamide	Packing film, catheters, sutures, mold parts

Considering a biodegradable polymer biomaterial to be different than that of the regular polymer biomaterial, the uses and implementations of this material has its advantages. There are a few methods as to how this biodegradation under goes a natural break down by hydrolysis or through enzymes, which lead to terms related to absorbable and identify biodegradation. The advantage of biodegradable biomaterials is the capability to have zero reaction with the body because of the materials ability to perform commensally with the human body to absorb the material completely without leaving any trace of material at the site. Also, some have been found to regenerate tissue due to the biodegradation process in response with the immune system. This tissue engineering can be used for surgical implants needed to treat or regrow tissue and help build bone through scaffolds.

Metallic Biomaterials

Metal alloys have been developed purposely for human use in the manufacturing of implants and devices. The body's tolerance to metals used to make alloys: iron (Fe), chromium (Cr), cobalt (Co), nickel (Ni), titanium (Ta), niobium (Nb), molybdenum (Mo), and tungsten (W) can only be endured by the body in minor amounts. Naturally, our bodies produce some of these

metallic elements that are essential for the body; iron is found in red blood cells, and cobalt is found in the synthesis of vitamin B-12, but it can be lethal in excessive amounts. The biocompatibility of the metallic implant is of considerable concern because these implants can corrode in a vivo environment [17]. The consequences of corrosion are the disintegration of the implant material, which will weaken the implant, causing the harmful effect of corrosion products on the surrounding tissues and organs [18].

316L Stainless Steel

316L stainless steel is a widely used and very common type of alloy necessary for implant applications. The letter "L" in 316L stainless steel accounts for the low carbon content of 0.03% for the composition throughout the bulk material. This inherently promotes the access of more chromium within the grain boundaries for better corrosion resistance. For the corrosion resistance, 316L stainless steel is a popular alloy because of its chemical composition of ≈18% Cr, ≈13% Ni and ≈3% Mo. Aside from its high resistance to corrosion, the mechanical properties are highly sought out after for load bearing implants. The elastic modulus of around 200 GPa for 316L stainless steel makes it an excellent candidate for bone implants capable of the high stress loading.

Electrochemical Treatment

A process referred to as reverse plating, the electropolish method uses a combination of a fixed current and a chemical electrolyte solution to remove unwanted flaws from the surface of a metal material. A low voltage of direct current (DC) is converted from an alternating current (AC) power source to maintain the constant current that varies on the voltage applied depending on the application or material. Lead, copper or stainless steel plates are used as a cathodic material that will react to the electrochemical process. The metal material being electropolished

is attached to rods made of titanium, copper, or bronze and is used to remove any flaws through an anodic reduction reaction. The concentrated acid electrolyte solution with a high viscosity acts as conductor that allows the metal material that is positively charged, anode, to release ions that will be attracted by the negatively charged, cathode. As the ions are removed from the surface of the material, oxygen in the form of gas is released and further aids in the cleaning process. Further benefits can be seen in Table 5.

Table 5: Benefits of electrochemical treatments [19]**.**

Electrochemical Process	Benefits
Electropolishing	Iron removal, enhances chromium/nickel for superior passivation, clean/smooth surface, polish inaccessible areas, leveling micro peaks, reduce part size
Magnetoelectropolishing	Enhanced pitting/corrosion resistance, reducing nickel leaching, shift corrosion potential positively, homogeneous passive layer, early biofilm formation

Magnetoelectropolishing is another electrochemical treatment used to remove flaws from the surface of a metal similar to the electropolishing process, but with an added parameter of applying an external magnetic field. The strength intensity of this magnetic field can alter the rate of dissolution by either enhancing or hindering this effect. Throughout the magnetoelectropolish process with a fixed potential, a Lorentz force is created as a cross product between the magnetic field and current. The effect this force causes is for the electrolyte to revolve around the axis parallel to direction of the magnetic field and this rotating movement decreases the thickness of the diffusive or viscous layer [20].

CHAPTER II

LITERATURE REVIEW

Development of Metallic Biomaterials

Metallic materials considered for medical implants have been in use since the 19th century, even more so when the era of the metal industry began to develop during the Industrial Revolution [21]. The demand for metallic implants was proposed due to the necessity for long bone repair. Since the early plea, metallic materials have dominated the area of orthopedic surgery and devices, including temporary and permanent devices [22]. Bearing in mind the industrial production of sizeable amounts of multiple metals and alloys, to that there is a limited success that is biocompatible and proficient enough to withstand the harsh environment for long-term acceptance as an implant material. Categorization of these materials can be placed into four groups grounded on major alloying elements: stainless steel, cobalt-based alloys, titanium-based alloys and miscellaneous others [23]. The United States Food and Drug Administration (FDA) has approved stainless steel, cobalt-based alloys, and titanium-based alloys in the array of medical implants made of these materials [24].

Biomaterial, Biomedical and Biological Materials

The word biomaterial with a prefix of "bio" relates to the biocompatibility than that thought to be biological or biomedical. Material science has identified a biomaterial to be a material engineered to work among a complex system and interact with a living system. Aside

from this definition and the many others that plague the field with different boundaries, a biomaterial is expressed as a component of a medical device, "any instrument, apparatus, implement, machine, appliance, implant, *in vitro* reagent or calibrator, software, material of other similar or related articles, intended by the manufacture to be used, alone or in combination, for human beings for one or more of the specific purposes of diagnosis, prevention, monitoring, treatment, investigation, supporting of sustaining life, control of conception, and disinfection of medical devices" [25].

Williams insinuated that biocompatibility covers all aspects of a bio-device function, including the interaction of cells and tissues with the implanted biomaterial [26][27]. Biocompatibility can be further categorized according to their ability to induce cell or tissue death (cytotoxic), cancer formation (carcinogenic), genetic damage (mutagenic), or blood clotting (thrombosis) [28][29]. The biocompatibility of a metal as a biomaterial is associated with the corrosion resistance and biological effects from the leaching of metallic ions.

Design of Metallic Biomaterials

The importance of the design and selection of a biomaterial varies on use of the medical application and specific location. The safety for long-term success without refusal from the human body will lead the metallic implant to require high corrosion resistance, relative mechanical properties, wear resistance, biocompatibility, osseointegration and cell proliferation.

Corrosion resistance. The human body's environment is physically demanding and chemically unforgiving on biomaterials. The most corrosion resistant stainless steels normally cause chronic allergy and toxic reactions in the human body, diagnosed after post-implantation period [30][31]. Although corrosion resistance affects the success rate of metallic implants, implants that perform excellent in one area of the body may suffer dramatically in another region

for the reason that various parts of the body have different pH values and oxygen concentrations. Human bodily fluids contain approximately 0.9% saline, Na^+ and Cl^- solutions, as the corrosion process is shortened by aqueous ions. However, the pH value of bodily fluid may fall into a more acidic concentration between 3-4 due to inflammatory cell secretion caused by surgery or injury [32]. Also, the internal partial pressure of oxygen is lower in the body and this lower oxygen count accelerates corrosion of metallic implants by slowing down the formation of protective passive oxide films on the surface [32]. Preferably, leaching of metallic ions should be diminished and remain low over the course of a prolonged period under normal physiological conditions.

Mechanical Properties. Natural bone is strong and tough, biomaterials need to mimic or match this mechanical property to the best of its ability. Young's modulus, ultimate tensile strength (UTS) and toughness are major mechanical properties sought out after as an importance to biomaterials. Stainless steel, cobalt-based alloys and titanium-based alloys dominate over other metallic alloys for their mechanical properties to experience substantial load bearing means with plastic deformation before failure. Dually noted that stainless steel, cobalt-based alloys and titanium-based alloys do have a much greater Young's modulus of over 100 GPa than that of bone, which is between 10-30 GPa [33]. These higher moduli of the alloys allow for the implant to withstand the entire load, but this can have some consequences toward the bone that does not bear a mechanical load surrounding the implant. The stress shielding effect would be caused from atrophy, biological response, and would require further surgery to repair. Therefor, any materials chosen to imitate bone would have a comparable Young's modulus or roughly closer.

Biocompatibility. No metal alloy is completely inert in the living body environment, the best selection process of metal alloy elements that currently exist and form naturally in the

human body. Common elements found in the human body average to approximately 96% of carbon, oxygen, hydrogen and nitrogen, the foundation for water and proteins [34]. The remaining 4% is composed of bone as minerals (calcium, magnesium, and phosphorus) or in blood and extracellular fluid as electrolytes (sodium, potassium, and chlorine) [35]. There are trace elements in extremely low quantities necessary for the suitable growth, development, and physiology of the human body, as it important that these elements stay at low levels because toxicity can occur at high levels [36].

Osseointegration. Osseointegration is a term that describes the process of new bone formation and bone regeneration, requirements in orthopedics [37]. The implants surface inability to bond to the surrounding bone and other living tissue due to micro-motions will cause the formation of fibrous tissue, which promotes loosening of the prosthesis [37]. Thus, it is crucial for the implant to have a suitable surface for surrounding bone to integrate with as surface chemistry, surface roughness and surface topography are factors to be considered for good osseointegration [38][39].

Stainless Steels

The benign nature of elemental iron has been perceived throughout history since the Iron Age, metal ion toxicity has been more recently studied [40]. Stainless steel is one of the many number of iron-based alloys that contain high amounts of chromium (11-30 wt%) and nickel [41]. Thus, stainless steel can be separated into two groups: chromium and chromium-nickel dependent on their chemical composition. Alternatively, they may be grouped into four factions based on their characteristic microstructures of the alloys: martensitic, ferritic, austenitic, or duplex (austenitic plus ferritic) [41]. However, austenitic stainless steel (type 316L) is used for implants [41].

Stainless steel has a minimal percentage of ~11 wt% of chromium, the amount enough to prevent the formation of rust from the atmosphere [41]. A few temporary implants that have used stainless steel has been fracture plates, screws, hip nails and for permanent devices would be a complete hip replacement. The chromium present in stainless steel has a positive attraction with oxygen to form a chromium rich oxide film (~2nm) and this surface layer is adhesive, which encourages self-healing [42][43]. Furthermore, nickel is the main alloying element that stabilizes the formation of austenitic in iron and contributes to the formation of oxide films from the alloys to enhance the corrosion resistance [41].

Stainless steel has had great accomplishments as a widely used alloy, but there are a few complications that present issues with long-term viability with highly corrosive bodily fluid produced in the human body. Majority of the devices in use are restricted to temporary implants such as internal fixations and hopefully the progressive research on the material will change that in the future.

Biocompatibility of Alloying Elements

There is three dominate alloying elements of 316L stainless steel: iron, chromium, and nickel, studying their biological performance connected with the leaching soluble ions or insoluble particles [44].

Toxicity of Iron. With the leaching of these iron ions throughout the blood, free ferrous iron reacts with peroxides to generate free radicals. This can be highly dangerous for it is very reactive and damages DNA, proteins, lipids, and other cellular systems. The typical effects of iron cause damage to the cells located in the heart and liver, causing adverse effects, which include coma, metabolic acidosis, shock, liver failure, coagulopathy, adult respiratory distress syndrome, long-term organ damage, and death if left untreated [45][46]. On average humans

experience iron toxicity above 20mg/kg of their total body mass and over 60 mg/kg is considered a fatal dose [47].

Toxicity of Chromium. Chromium has a multitude of possible oxidation states, Cr^{3+} and Cr^{6+} are the most frequent concentrations and the toxicity depends on which oxidation state. The effects of toxicity and carcinogenic properties of hexavalent chromium (VI) have been under study while water insoluble trivalent chromium (III) are not considered to be an immediate health hazard [48][49]. Chromate dust has carcinogenic properties that have been related to increase risk toward cancer [50]. Any contact with chromate may lead to allergic contact dermatitis and irritant dermatitis, resulting in skin ulcers [51].

Once chromium has entered the living system, chromium (VI) is reduced to chromium (III) throughout the blood before entering the cellular structure and is then excreted out of the body through urine. Some studies have shown that high concentrations of chromium (III) in the cellular system may lead to damaging effects in DNA [52][53]. The effects of chromium (VI) are indicated by the strong oxidative properties; once within the blood stream it will damage the kidneys, liver and blood cells through the oxidation reaction, the end result being renal and liver failure due to hemolysis [48].

Toxicity of Nickel. The U.S. standard to minimalist risk level of nickel and its compounds is 0.2 $\mu g/m^3$ of inhalation between 15-364 days [54]. A few respiratory diseases caused by toxicity of nickel include acute pneumonitis from nickel carbonyl [24], chronic rhinitis and sinusitis, cancers of nasal cavities and lungs [55]. Nickel carbonyl, $Ni(CO)_4$, are volatile gases, while fumes of nickel Ni_3S_2 is known to be carcinogenic and cause cancer in the lungs [56]. The mechanism, which makes nickel harmful, is the active uptake by cells across their membranes (endocytosis) and the nickel compounds with the ability to be endocytosed include

their crystalline nature, negative surface charge, 2-4 μm range particle size and low solubility [57]. As the nickel compound particles are endocytosed by target cells, the vesicles are acidified by fusion with lysosomes and Ni^{2+} is released [58]. Deleterious changes, the formation of oxygen radicals and subsequent DNA damage is possible, a known mechanism for initiation tumorigenesis [59].

316L Stainless Steel Alloy

316L stainless steel is one of the most adequate metallic biomaterial and is widely used in devices of short and long term implants due to its ease of fabrication with a relatively low cost [60]. Considering the alloy to be widely used in medical devices of orthopedic, intravascular, dental applications [61]: this increasing trend is responsible because of its high mechanical strength, excellent corrosion resistance, good processability and biocompatibility [62]. The properties possessed by the alloy have issues when within close proximity of human tissue or fluids. While the US Food and Drug Administration has approved 316L stainless steel, the use of this alloy still does have its issues with the environment in which it is in contact with the human body [63][64]. The concern has always been apparent of both permanent or temporary implants because of the resulting effects of the individual metal elements [65]. The toxicity of a few elements such as chromium, Cr (VI), and nickel, Ni, are highly toxic against the human body and may potentially lead to the cause of cancer (carcinogenic). A few methods are in implementation to relieve the effects caused from leaching ions in the circulatory system already as a considerable amount result in surface treatments or modifications.

Due to the characteristic of leaching ions from these elements, corrosion resistance is a factor of immediate concern for the biocompatibility. Among the properties, corrosion is an important issue toward implants in human tissue for devices in close contact with bodily fluids

[66]. Corrosion plays an important role for biocompatibility and the response of the body to accept of deny the implant. The ion bi-products of 316L stainless steel such as iron (Fe), chromium (Cr), nickel (Ni) and molybdenum (Mo) can eventually cause a build up or accumulation around the surrounding tissue or be transported through the blood stream across various parts of the body [67].

The surface of the stainless steel will generate a thin film layer of oxide and hydroxide when exposed to the ambient environmental air conditions [68]. The thicknesses of the layers range from 10-15Å from the surface of the bulk material and are not chemically stable [69]. Naturally the formation of the thin layers will combat the effects of leaching ions, but the resilience is even not enough for short-term implants. Considering their instability and potential reaction while attempting to modify the surface characteristics, it would be best to remove any of these oxides and hydroxides by chemical treatments to obtain an ideal surface to efficiently interact with the body functions.

Surface Treatments of 316L Stainless Steel

The threat at which stainless steel affects the body has researchers developing new methods of surface treatments on one of the first materials introduced as an implant for the body. There have been numerous methods to fabricate films, coatings, or chemical modifications to retard the rate at which ions are released from the metal. The innovation on a metal that has provided results and data over decades of research needs new ingenious techniques to further allow the competitive edge against new materials. The criticality at which treatments can react well with the human body may be derived from the corrosion resistance to gain the biocompatibility needed to create an enhanced level of protection. Treatments in production include chemical treatments, mechanical treatments, chemical etching, acid dipping,

hydroxyapatite coatings, ceramic Nano-composite coatings, thermal treatments, laser surface melting, and plasma exposure to name a few of many. The reason behind these techniques is be able to create a passive chromium oxide layer and the increase of that film thickness.

Surface properties of metallic implants play an important role in their biocompatibility, functionality and with safety in mind [70][64]. Consequently, different approaches to efficiently acquire the best surface texture, energy and chemistry of implants [71][72]. One way to minimize the release of corrosion products from the implant to the surrounding tissues is to apply protective coatings [60]. Another technique has been the use of film deposition in order to modify the alloy's surface for the reason that the thin film has a superior corrosion resistance [66]. And among the sophisticated multitude of surface treatments, electrochemical manipulating the surface has been considered a promising technique to endure the corrosion resistance and biocompatibility of implants under physiological conditions [73][74].

Electrochemical Process

The electrochemical process has been around for ages and after the turn of a century with it in use it is one the most popular application in achieving necessary results for electropolishing. A Russian chemist, E. I. Shpitalskii, was interested in this process and held patents for his inventions in the early nineteen hundreds in Germany and Russia. As this widely used process is currently used, the steps towards the many theories we test today started when P. Jacquect and H. Figour electropolished nickel in a perchloric-acetuc acid solution. With the theories wide spread about varying electrochemical processes the parameters have a range of several variations which makes each theory different based on the result's requirement. Whether there is a definite electrochemical that is commonly used is hard to postulate considering the theories very based on the parameters. The benefits of this process are pronounced to be used on sophisticated

technological advanced applications because it stipulates a smooth, uncontaminated, Beilby layer free [75], corrosion resistant surface. Along with new processes and techniques, magnetoelectropolishing paves way toward a new process of possibilities.

Research and development on the electrolyte solution bath has under gone new interest for further alloys and metals. The electrolyte solutions that have yielded the best results are perchloric acid and perchlorates, but only for laboratory use instead of on an industrial scale because of the possibility of a reaction creating an explosion. Although, there is an industry standard as to an electrolyte solution, phosphoric-sulphuric acid, that is frequently used in the electropolishing of austenitic stainless steels.

The theory of Hoar suggested the nature of the surface film formed during electropolishing [76]. This thin passive film initiates the removal of material from the surface. As the film is formed on the anode the progressive electrolyte does not allow the thin passive film to increase on the surface as it is disintegrates after being created. This solid film theory in turn dissolves the metal's surface into the oxides and not toward the electrolyte solution; the benefit of this is avoiding the crystallographic etching [77]. The metal ions are dispensed into the oxides and the process of dissolution of those oxides is introduced in the electrolyte. The current density plateau is a major factor on whether or not the presence of oxygen is formed from the above process. Performing electropolishing above the current density plateau under oxygen evolution regime supports the presence of oxides; the bare metal surface does not promote this evolution of oxygen [77]. The conceptual theory of smoothing the metal's surface is derived from the Jacquet's viscous layer. Between the electrolyte and thin film exists the viscous layer in which the peaks are exposed at a lesser amount resulting in a higher current density leading to a quicker dissolution.

The viscous film theory suggested by Jacquet is a mechanism of smoothing the surface of the metal during the electropolishing process. The method at which the theory is proposed is the expendable ion released during the dissolution will adhere to the surface, creating a resistance to lower the current and speed up the dissolution process. Its thickness is not distributed over the entire surface as the protruding peaks and valleys will carry a varying electrical resistance, the viscous layer at the peaks is considerably thinner and the electrical resistance is lower and allows the removal of material rapidly. Divergently, the valleys are engulfed in a thicker viscous layer with a higher resistivity and dissolution rate decreases; results of these concentrated differences of the viscous layer within the protrusions and depressions yields a leveling effect [77]. The legitimacy of these theories can be assessed due to the correlation between the voltage applied and current density, the voltage density curve (V-I) is key to be able to determine the ideal conditions at which the electrolyte solution will coincide with the metal being analyzed. The best electrolyte solution is achieved in the range of the current density plateau and austenitic stainless steel in phosphoric-sulphuric acid obtains the best results above or below the oxygen evolution regime.

As stated above, electropolishing has been used commercially over the years for medical application and has been studied over decades to achieve the results per theories for individual metals. The passivation properties that exist with electropolishing are unique in creating an oxide layer. This passivation created from the surface oxide layer could be enhanced by adjusting the thickness, morphology, or chemical composition by means of different treatments [20]. The electropolishing process with the use of an externally applied magnetic field provides the surface with new properties and better characteristics of microroughness, hydrophilicity, corrosion resistance and oxide film morphology [78][79]. The external magnetic field will also minimize

the microtopography by decreasing the microroughness and minimizing the surface area on the macro and nano scale [80][81]. This process to incorporate a magnetic field complicates the system at which electropolishing already has with options of modifying multiple parameters. The externally applied magnetic field, a process that could ideally exhibit the reduction of microroughness, better surface wetting, increased surface energy, reduced and more uniform corrosion resistance, minimization of external surface staining and improved cleanability in shorter time frame [82]. The oxide films formed on the surface of a metal are essential for the biocompatibility and hemocompatibility of implants or devices. Surface characteristics vary depending on the treatments and influence biological effects. The stability of the surface oxide layer directly influences and impacts the biocompatibility of a material, a barrier to block the release of ions from the retaining material under the protective surface [64].

The electrochemical reaction from an externally applied magnetic field can be divided into three classifications: electron transfer, mass transfer (Lorentz Force), and morphology and chemistry of the treated material's surface is dissolved [83]. A process that can alter the rate of dissolution dependent on the strength at with the magnetic field is applied [83]. A possible process incumbent by the magnetic field interloping with the electron structure and the adjustment of the polarization of the free surface electrons [83]. A Lorentz force is created; cross product of the magnetic field and current, performed under a fixed potential mode follows the normal diffusion principle [83]. This force rotates the electrolyte solution around the axis parallel to the direction of the magnetic field and the rotation of this electrolyte will impede the thickness of the viscous layer [83]. In theory, this process should speed up the dissolution by increasing the rate of mass transport and is due to the reduction of the thickness [83].

Varying Conditions

Studies of better understanding and improving the process that electropolishing and magnetoelectropolishing have provided researchers is on going to further improve methods on 316L stainless steel. The abundance of applications of 316L stainless steel as a biomaterial for its versatility is worth investigating [84][85] further for the properties it posses' with these new advances. Previously stated, any up to date literature data does not provide an inclusive set of dependences between the electropolishing conditions and the results of the process [85][64].

Hryniewicz *et al.* investigated the difference in changing the current density during the electrochemical process affects the conditions of the surface film layer created by iron and chromium on the plateau level. X-ray photon spectroscopy (XPS) was used to understand the changing conditions of the electropolishing process and depict any metallic, oxide, or hydroxide films detected on the surface that may detour the biocompatibility of 316L stainless steel. The results indicated that the surface treatment, whether electropolished or magnetoelectropolished, gains substantial differences of Fe 2p in the XPS analysis [86]. On the other hand, chromium Cr had less of a differentiating impact from all the surface treatments [86]. Increasing the current density to 200 A/dm^2 or higher during electropolishing yielded ineffectiveness to form an advantageous surface film [86][87]. The effectiveness of the magnetic field intensity was found to be at 350 mT and as increasing beyond this intensity, produced results of an increase in the Lorentz force that converts the laminar convective flow of the electrolyte into a turbulent flow [86][87].

In earlier results presented by Hryniewicz *et al.*, a proprietary electrolyte solution and parameters were used to acquire some unique results. A magnetic field of 500 mT was used in the magnetoelectropolish samples and absent in electropolish samples during at which the

electrolyte bath was unstirred with a temperature between 66-69 °C. The corrosion studies in an open circuit potential (OCP) revealed a start to a higher potential of 180 mV with its value increasing to 240 mV in a 24 h time period for the magnetoelectropolished sample [82]. As for the electropolished sample, the initial open circuit potential started at 168 mV and plateaued roughly below 200 mV after the 24 h time period, a worse performance as apposed to magnetoelectropolishing [82]. The XPS analysis for the treatments revealed the increased levels of oxygen due to oxides, along with other elements such as calcium, sodium, and phosphorus with a vanishing nickel substrate [64]. As for the magnetoelectropolishing, the characteristics showed high amounts of oxides with lower amount of iron and chromium compounds present [82]. Some drawbacks have presented themselves with the use of a magnetic field at higher potentials. As the electropolishing process of 316L stainless steel had an increasing quantity of oxides and hydroxides, the addition of the magnetic field contributions was an improvement to the electropolishing system. An advantage found in both processes has exhibited phosphorus, non-metal, on the surface of 316L stainless steel to possibly be used on this biomaterial. As with disappearance of metallic chromium and iron, changes in the chemical composition became apparent with the formation of oxides and hydroxides after the magnetoelectropolishing. With the applied magnetic field during electropolishing, leaching of selective elements of iron and nickel were drawn away from the surface layer. What can be determined from this study is the positive sustainability of the affects from a magnetic field on the electropolishing process to be an improved performance on 316L stainless steel as a biomaterial [82].

316L Stainless Steel Stents

The number one cause of death in countries worldwide is caused from coronary artery disease as a result from the build up of plaque [88][89]. This phenomenon deemed coronary

artery disease (CAD) has high mortality rates in the Western world [90][91]. On the average of 400,000 patients are treated annually in the United States to battle coronary artery blockage [92]. Occlusion of coronary arties has a typical attribute of the build up of fatty deposits or calcified plaque, atherosclerosis, under the inner lining of the blood vessel [93]. Stents are used to help alleviate the blockage from coronary artery disease, they are metallic lattice structured cylindrical tubes made of 316L stainless steel [94]. The reason stainless steel is the material of choice for stents is because of the better mechanical properties, plastic formability and good corrosion resistance [95]. However, thrombosis, blood clotting, is related to stent implantation [96] and is triggered by the activation of the intrinsic coagulation system as the plasma and platelets adhere to the surface in the early stages of stenting [97].

Several blood serums such as fibrinogen, albumin, and immunoglobulin absorb themselves directly on the surface of the stent within minutes of implantation that does evoke agglomeration of blood platelets [98]. A thick vascular media of smooth muscle cells bounded by fibroblast and collagen bundles exists within the blood vessel surrounding the inner monolayer of endothelial cells [99]. The endothelial cells discharge a monitoring system of molecules to regulate the vascular tone of the blood vessel, permeability, inflammation, and thrombosis [100]. The level or degree of thrombocytes depends on the surface properties of the material of the adhesion of fibrinogen and platelet attachment [101]. Passive films on the surface of the material are important in influencing thrombosis because of the electrochemical nature of blood and metallic implants [102]. The steady availability of re-endothelializatoin along the artery wall and endothelialization on the stent after being implanted is of immediate importance [103].

Recent studies from researchers have attempted to modify the stent's surface in hopes of minimizing rejection of problematic issues [104]. The goal of creating a passive layer on the 316L stainless steel surface will help combat these difficult situations and generate a more positive response for cell proliferation. Several studies have divulged the effective surface properties that impact cellular behavior [105][106]. A promising development as a surface modification would be coating or films on the material's surface to alter the properties in favor of cell viability without meddling with the implant's main functionality [107].

Bioactivity

In a study conducted by Habibzadeh *et al.*, iridium and titanium oxide coatings of multiple concentrations ($Ir_{0.2}Ti_{0.8}$, $Ir_{0.4}Ti_{0.6}$, $Ir_{0.6}Ti_{0.4}$, $Ir_{0.8}Ti_{0.2}$) were formed on 316L stainless steel. The study was directed towards the reaction of platelets and endothelial cells in contact with these oxide coatings to determine the biocompatibility. Platelet adhesion is a crucial event leading to the formation of thrombosis [108] and any preventative method should be considered. The study did yield a decrease of platelet attachment by nearly 85% on the $Ir_{0.2}Ti_{0.8}$ oxide surface, a remarkable improvement of blood compatibility [109]. The thrombosicity was decreased by employing a coating with 20-40% Ir [109], the agglomeration of platelets on these coatings ratios were significantly lower than the other concentrations. The interaction between the coatings and platelets could very well be affected by the wettability, in the case of hydropholicity. This case combined with surface roughness and surface chemistry may control the outcome of platelet accumulation [109]. On the other hand, cell adhesion of endothelial cells is a positive necessity for viability and cell proliferation. There was a major increase in the endothelial cell bond toward the oxide coatings when the iridium concentration was higher than the titanium concentration [109]. This can be assessed in other investigations that pure iridium

oxide on a surface has high biocompatibility and radiopacity for the modification of stent material [110]. Another observation was concluded that the incubation time for endothelial cells had an important gestation period during the first 2 hours, as there were no substantial differences between the 2-4 hour incubation time [109]. The overall interaction between platelets and endothelial cells with iridium/titanium oxide surface coatings led this study to conclude the 20% and 40% of iridium yielded minimal interaction with platelets along with higher endothelial cell attachment [109] and from a previous study, $Ir_{0.4}Ti_{0.6}$ was found to be more corrosion resistant [111]. Overall, the choice for a iridium/titanium oxide coating with a composition of $Ir_{0.4}Ti_{0.6}$ for coronary stents would sufficiently abide by the biocompatibility and hemocompatibility [109].

Research Objective

Corrosion resistance controls the success rate of a metallic implant and is a formidable characteristic of stainless steel. The leaching ions from these implants have a volatile reaction toward living tissue and body system, causing long-term complications. In a method to overcome the problem, different electrochemical surface modifications were carried out without any changes toward the bulk properties of 316L stainless steel. The proposed surface modifications affect the surface chemistry, morphology, wettability, corrosion resistance and biocompatibility. The surface treatments should undergo the following effects on implants:

- Corrosion resistance improvement □
- Reducing leaching of ions
- Generate a stable oxide film □
- Reduce cytotoxicity □
- Cell implant adhesion and proliferation □

Research Methodology

The plan to follow the research methodology requires the selection of materials and their treatments i.e. 316L stainless steel: above electropolish, below electropolish, above magnetoelectropolish, below magnetoelectropolish. The surface characterization will be carried out with the scanning electron microscopy (SEM) and Energy dispersive X-ray spectroscopy (EDS) for the analysis of surface chemistry. The atomic force microscopy (AFM) was conducted in order to study the minute roughness changes on a nanometer scale. The surface wettability studies were completed on a Kyowa contact angle meter. The electrochemical behavior of the alloy was studied before and after each surface modification. Potentiodynamic cyclic polarization scans were acquired to understand the corrosion vulnerability of each treatment. The biocompatibility and cytotoxic assays were conducted with the use of pre-osteoblast MC3T3 cells and human umbilical vein endothelial cells.

CHAPTER III

MATERIAL AND EXPERIMENTAL METHODS

Material

The commercial grade availability of 316L stainless steel was obtained in the form rods with a chemical composition of the main alloying elements shown in Table 6.

Table 6: Chemical composition of commercial grade 316L stainless steel (wt%)

C	Mn	Cr	Ni	Mo	N	Fe
0.03	2.00	17.0	11.5	2.00	0.02	Balance

Material Preparation

The commercial grade s316L stainless steel rods were cut with a high-speed grinding saw into circular coupons, the coupons having a thickness ranging between 0.25 and 0.33 of an inch in diameter. The coupon surfaces were ground on both faces using silicon carbide grit paper on a Buehler® abrasive belt grinder. The paper grit sizes of 240, 320, 400, 600, 800 and 1200 were used simultaneously in order from the lowest to highest abrasiveness to achieve a smooth and mirror like surface finish. Then, each sample went through a cleaning process with deionized water and afterwards an ultrasonic cleaning with ethanol for 15 minutes.

Surface Treatment

The mechanically ground coupons were sent to Electrobright® (Macungie, PA, USA) for electrochemical treatments. This company performed electropolishing (EP) in 500 ml plastic beakers and magnetoelectropolishing (MEP) in 500 ml plastic beakers inside four ceramic ring

magnets (magnetized through their thickness) stacked together with a magnetic field of approximately 100 mT (millitesla). For each treatment, the coupons were either above or below the oxygen plateau. The above oxygen evolution conditions were as followed: electrolyte solution of 700 ml 85% H_3PO_4 (phosphoric acid) with the addition of 30 ml 66B° H_2SO_4 (sulfuric acid), voltage of 10 V, temperature at 60 C°, time of 5 min. and a Cu (copper) cathode was used to complete the circuit. The below oxygen evolution conditions were as followed: electrolyte solution of 200 ml 66B° H_2SO_4 (sulfuric acid) with the addition of 800 ml CH_3OH (ethanol), voltage of 10 V, temperature at 25 C°, time of 5 min. and a Cu (copper) cathode was used to complete the circuit.

Surface Characterization

The morphology on the coupon surface was analyzed by a scanning electron microscopy (SEM) (Sigma VP Carl Zeiss, Germany). Energy dispersive spectroscopy (EDS) (Carl Zeiss, Germany) was used to examine the elemental distribution on the alloy's surface. The chemical composition was investigated with the use of a k-alpha x-ray photoelectron spectrometer (XPS) (Thermo Scientific, USA). The surface roughness, with the tapping mode covering an area 20 μm x 20 μm, was analyzed with an atomic force microscopy (AFM) (Nanoscope IV MultiMode, Digital Instruments, USA). The interfacial free energy, contact angle, surface free energy and work of adhesion were examined by expending the sessile drop method using the Kyowa angle meter (DM-CE1, Japan).

The surface chemistry was analyzed with a Thermo Scientific Model K-Alpha XPS instrument by X-ray photoelectron spectroscopy (XPS). The XPS spectra were recorded using a monochromatic Al Kα source (1486.67 eV) with a variable spot size (i.e., 30-400 μm) and an electron take-off angle of 90°. The typical base pressure is 2×10^{-9} mbar or lower. Survey spectra were recorded in a range of 0-1350.0 eV with a pass energy of 200 eV, step size of 1.0 eV and

dwell time of 10.0 ms. High-resolution spectra were acquired for O 1s, Cr 2p, Fe 2p and Ni 2p regions collected in the fixed analyzer transmission mode with a pass energy of 10.0 eV, step size of 0.1 eV and dwell time of 50.0 ms. Binding energies in survey and high-resolution spectra were calibrated with respect to the C 1s peak at 285.0 eV. The acquired data was collected and processed using the Thermo Scientific Avantage XPS software package. Peak fitting was performed using mixed Gaussian/Lorentzian peak shapes and a Shirley/Smart type background. Depth profiling analyses were conducted with a Thermo Scientific EX06 argon ion gun operated at 1000 eV and rastered over a 2 mm x 4 mm area. Sputtered depths were calibrated with a 100 nm SiO_2/Si standard.

Corrosion Experiment

The corrosion study was assessed with an electrochemical test, the samples were encapsulated within a glass cell as shown in Figure 2. A phosphate buffer saline (PBS) with an average pH range of 7.4 in a humidified atmosphere with a temperature of 37 °C and a 5% CO_2 (Sigma Aldrich) concentration was followed by ASTM standards: G102-89 (97), ASTM: G3-89 (98) and ASTM: G31-72 (99) to be used as an electrolyte. The PBS was purged with pure nitrogen (99.9%) gas for 15 minutes before testing. The test was performed on a GAMRY potentiostat (reference 600) with a polarization cell setup consisting of the electrolyte (PBS), graphite rod for the counter electrode, saturated calomel electrode SCE (+0.242 V vs SHE) for the reference electrode and 316L stainless steel for the working electrode condensed within a electrochemical cell as shown in Figure 1. The potentiodynamic polarization curves were acquired with a constant voltage scan rate of 1.0 mV/s. The Gamry Framework and Gamry Echem Analyst software was used to extract the corrosion data. ASTM standard F2129 for the cyclic potentiodynamic polarization testing was conducted for the studies.

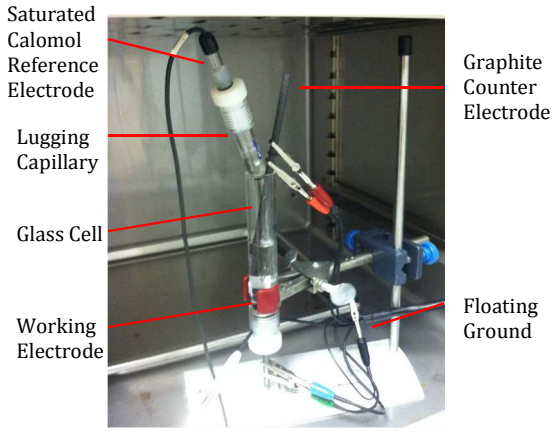

Figure 1: Electrochemical cell

Cell Viability

An MTS assay (G3580, Celltiter 96® AQueous One Solution Reagent, Promega Corporation) was evaluated to determine how the metal ions leached from the316L stainless steel coupons affected the percentage a viable MC3T3-E1 pre-osteoblast cells (ATCC® CRL-2A593TM) and human umbilical vein endothelial cells (ATCC® PCS-100-010) in ionized media concentrations. The cells were cultured in MEM alpha modification media (Thermo ScientificTM HyCloneTM SH3026501) concentration containing 10% fetal bovine serum (FBS) (Thermo ScientificTM HyCloneTM SH3008803HI) with 1% Penicillin-Streptomycin (Sigma-Alridch P4333) for the MC3T3-E1 pre-osteoblast cells and vascular cell basal medium (ATCC® PCS-100-030) concentration containing an endothelial cell growth kit –BBE (ATCC® PCS-100-040) with 1% Penicillin-Streptomycin (Sigma-Alridch P4333) for the human umbilical vein endothelial cells in a humidified atmosphere with a temperature at 37 °C and 5% CO_2 air quality mix. The 316L stainless steel coupon surfaces were exposed to both the MEM alpha modification media and vascular cell basal medium for 12 days with a 3 day interval period at which it was collected. 20,000 cells were counted by using a hemocytometer and then retained in a 96-well plate with 200 µl of growth media per well. Then, the cells were incubated for 24 hours

period to allow them time to attachment to the well plate surfaces. After another 24 hours of incubation, the growth media was replaced with growth media/ions concentration (100%) that was exposed to 316L stainless steel surface. A few culture wells with cells were used with only growth media as control. Again, the cells were incubated for another 24 hour period and afterwards 100 µl of ionized media was removed from the wells containing cells to be replaced with 20 µl per well of Celltiter 96® AQueous One Solution Reagent. The culture plate was then placed in the incubator for a 4 hour period and immediately removed to acquire the optical density measurements, recorded using ELx800TM BioTek absorbance microplate reader controlled by Gen5 software with a 490 nm absorbance excitation filter.

The cells were cultured in MEM alpha modification media (Thermo ScientificTM HyCloneTM SH3026501) concentration containing 10% fetal bovine serum (FBS) (Thermo ScientificTM HyCloneTM SH3008803HI) and 1% Penicillin-Streptomycin (Sigma-Alridch P4333) in a humidified atmosphere with a temperature at 37 °C and 5% CO_2 air quality mix. 30,000 cells were seeded onto each surface along with 200 µl of growth media for complete covered in a glass cell as shown in Figure 2. After a 24 hour incubation period, the cell staining was achieved using NucBlue® Live Cell Stain Ready ProbesTM (R37605, Invitrogen Inc.) in order to stain the cell nuclei and MitoTracker Red (M7512, Invitrogen Inc.) in order to stain the mitochondria. Overlay fluorescent images of both stained nuclei and mitochondria were captured using the EVOS® FL Cell Imaging System (AMF4300, Invitrogen Inc.).

Other cells were cultured under the same growth conditions and 50,000 cells were seeded onto each surface along with 200 µl of growth media for complete covered for a 3 day incubation period in glass cells as shown in Figure 2. On the final day before SEM images were acquired, a cell fixation protocol was followed to attach (90% glutaraldehyde/10% DPBS) and dehydrate (

30%/70%, 50%/50%, 70%/30%, 90%/10% ethonal/ DI H_2O) the cells in a series of chemical solutions, immersed in hexamethyldisilazane (DHMS), and wash baths (DPSB/MODIFIED (Thermo ScientificTM HyCloneTM SH30028.02)).

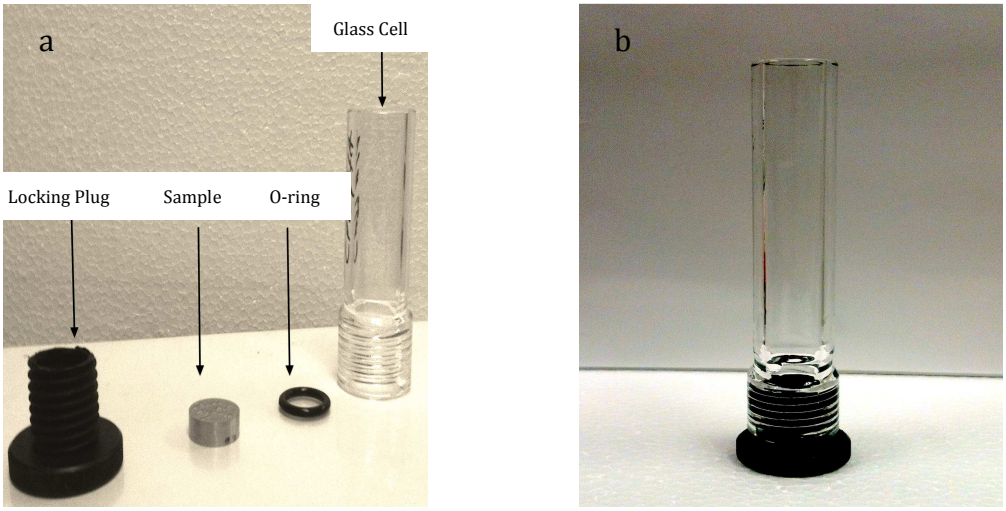

Figure 2: Glass cell used in corrosion and direct cell studies: (a) unassembled glass cell, (b) assembled glass cell

CHAPTER IV

RESULTS AND DISCUSSION

Surface Characterization

Surface treatments offer a competitive method to altering the surface chemistry of an implant's surface in order to enhance the properties of the corrosion resistance and the biocompatibility at which these implants are used in biomedical applications. Being able to modify the surface with specific treatments will enable the user to apply implants in necessary locations in order to protect the human body as a precautionary measure without completely changing the biomaterial's bulk properties. Some of these treatments are an advantage to help control major factors that cause damaging effects to a biological system and a few of these treatments can be chosen to keep 316L stainless steel corrosion resistant and biocompatible with the human body.

The interactions between human blood, tissue, fluids, cells, and proteins dictate the biological responses the body has toward the implant. To effectively succeed at obtaining a substantial surface treatment, many of the biomaterial's physiochemical properties will be drawn from the surface topography, wettability, morphology, and chemistry. Figure 3 represents the surface morphology of the material and elemental chemistry distribution information of 316L stainless steel with their respective treatments compared to the untreated (UNT) sample. Each surface treatment was observed for above and below oxygen for both electropolishing and magnetoelectropolishing. As there are no visual variations between the different surface

topographies of the four treatments, the main depiction of the chemical composition will be investigated as the alloying elements are of concern for creating a stable surface oxide film. Considering UNT to be the control, the assumption of natural formations of oxides may be created as the surface is exposed to atmospheric air conditions. The nature of oxygen's electronegativity, results in the formation of stable chemical bonds with elements to formulate corresponding oxides. As mentioned, 316L stainless steel surface will naturally create a solid oxide barrier through passivation between a few alloying elements. What is attempting to be achieved is an increased formation of this passive oxide films in order to increase the corrosion resistance and further encompass other parameters that are dependable to each other for a sustainable implant. Figure 3 reveals the weight percentage of all the treatments with no to little noticeable difference between the main alloying elements of iron, chromium, and nickel, as these can be beneficial with the formation of oxides. The weight percentage for the alloying elements under these high percentiles would be categorized under the combination of a close proximity to oxide film and bulk material, as the EDS analysis revealed no weight percentage of elemental oxygen. This may be because the intensity at which the electron beam penetrates the surface will etch through the complete surface oxide film and will only expose trace amounts of oxygen distributed with its corresponding elements and begin to bare the chemical composition of the bulk properties. This presence of oxygen is a significant constitute for reducing the corrosion by increasing the resistance to the dissolution of ions released from the surfaces. The results will be further analyzed with x-ray photoelectron spectroscopy (XPS) to characterize the formations through peak fitting of oxygen and 3-D high resolution spectra of iron, chromium, and nickel oxides on the surface.

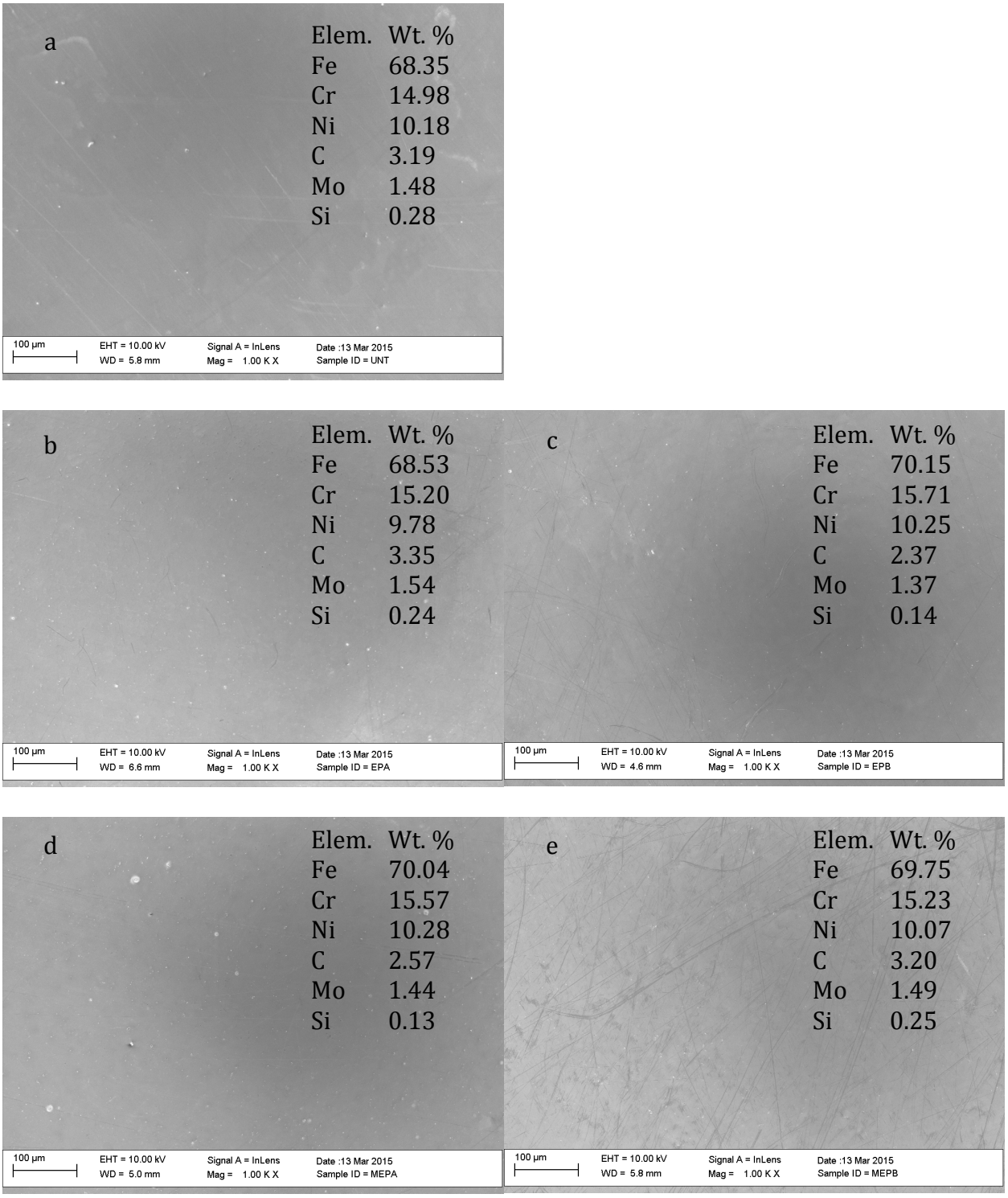

Figure 3: SEM & EDS of 316L stainless steel: (a) UNT, (b) EPA, (c) EPB, (d) MEPA, (e) MEPB

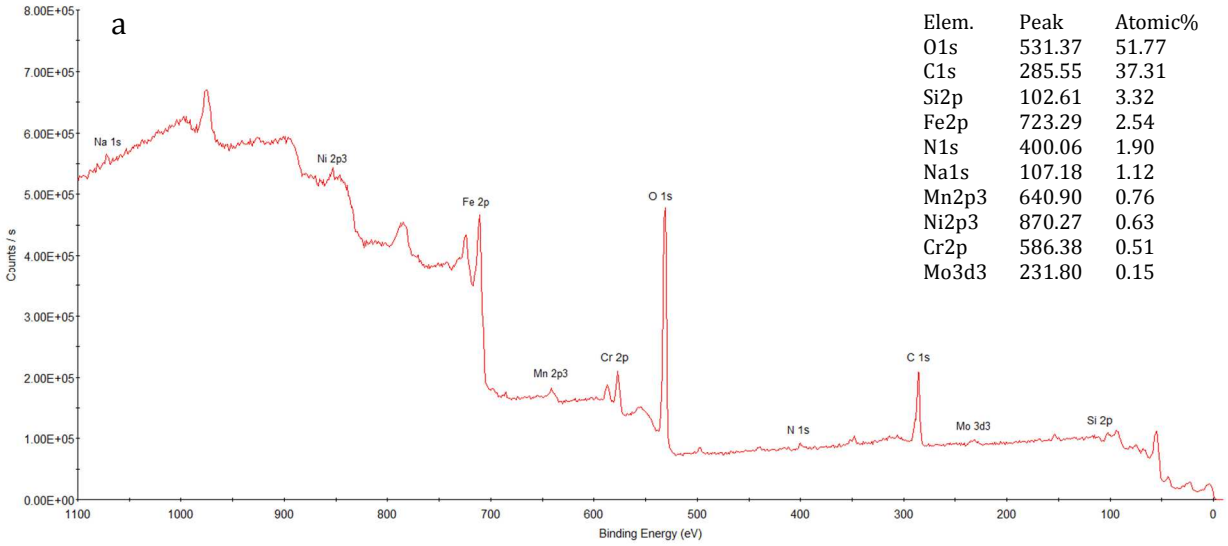

Elem.	Peak	Atomic%
O1s	531.37	51.77
C1s	285.55	37.31
Si2p	102.61	3.32
Fe2p	723.29	2.54
N1s	400.06	1.90
Na1s	107.18	1.12
Mn2p3	640.90	0.76
Ni2p3	870.27	0.63
Cr2p	586.38	0.51
Mo3d3	231.80	0.15

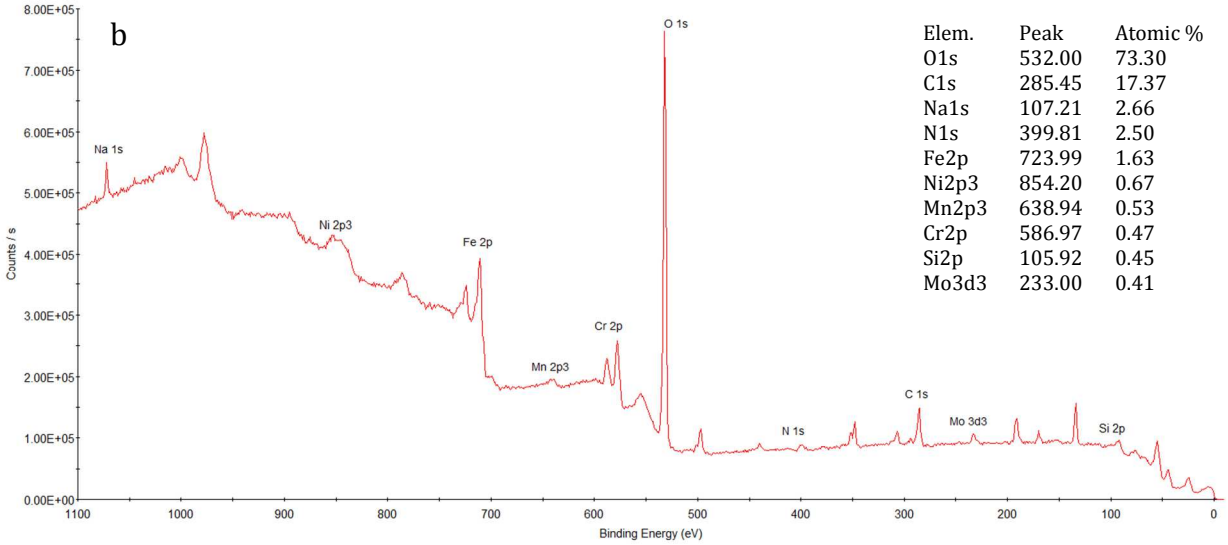

Elem.	Peak	Atomic %
O1s	532.00	73.30
C1s	285.45	17.37
Na1s	107.21	2.66
N1s	399.81	2.50
Fe2p	723.99	1.63
Ni2p3	854.20	0.67
Mn2p3	638.94	0.53
Cr2p	586.97	0.47
Si2p	105.92	0.45
Mo3d3	233.00	0.41

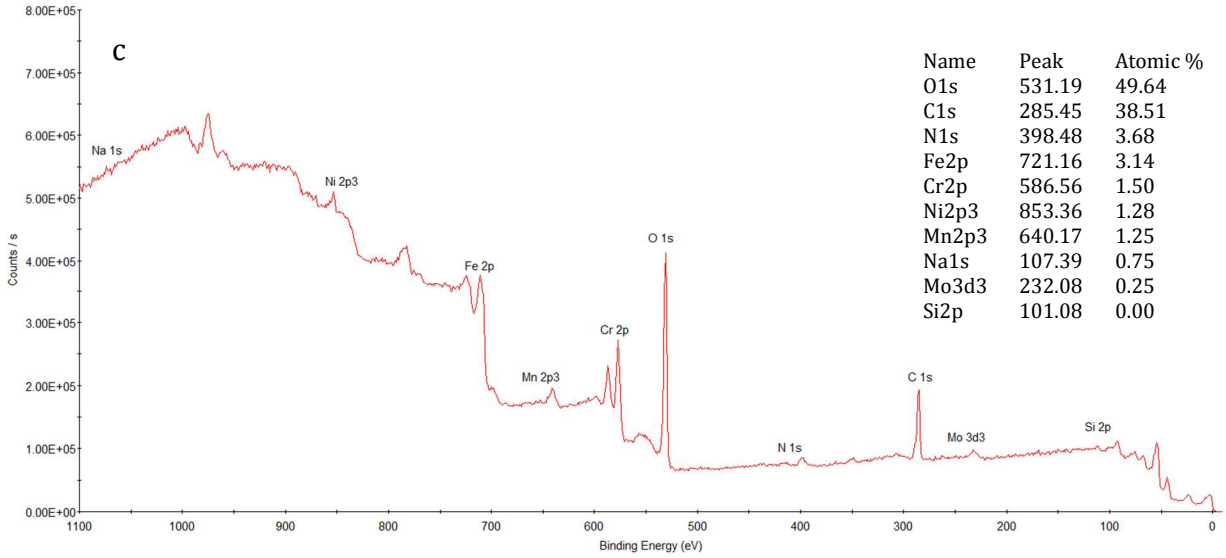

Name	Peak	Atomic %
O1s	531.19	49.64
C1s	285.45	38.51
N1s	398.48	3.68
Fe2p	721.16	3.14
Cr2p	586.56	1.50
Ni2p3	853.36	1.28
Mn2p3	640.17	1.25
Na1s	107.39	0.75
Mo3d3	232.08	0.25
Si2p	101.08	0.00

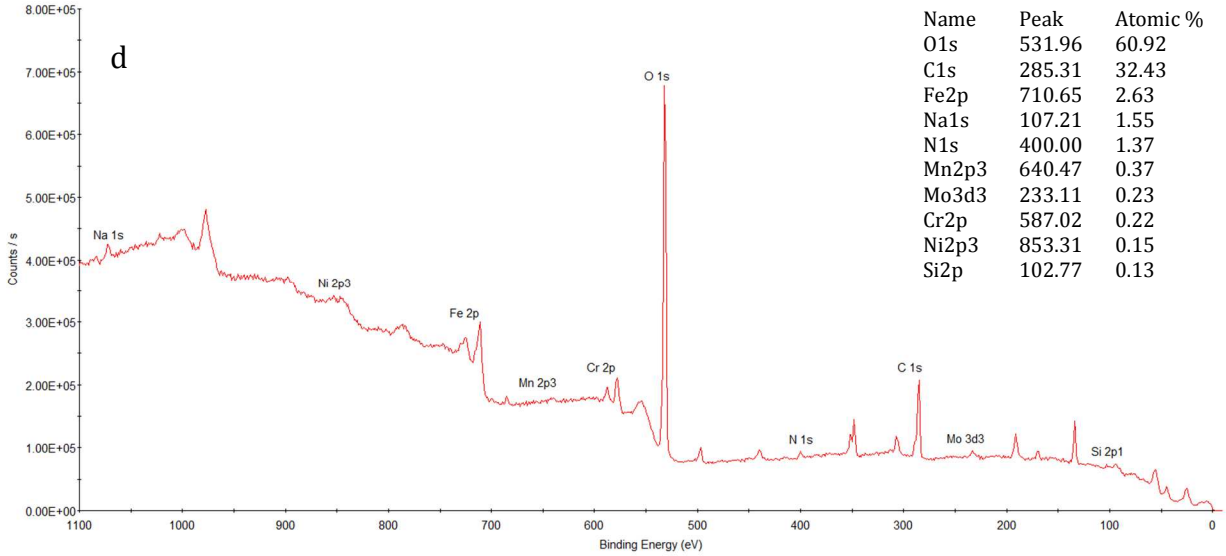

Name	Peak	Atomic %
O1s	531.96	60.92
C1s	285.31	32.43
Fe2p	710.65	2.63
Na1s	107.21	1.55
N1s	400.00	1.37
Mn2p3	640.47	0.37
Mo3d3	233.11	0.23
Cr2p	587.02	0.22
Ni2p3	853.31	0.15
Si2p	102.77	0.13

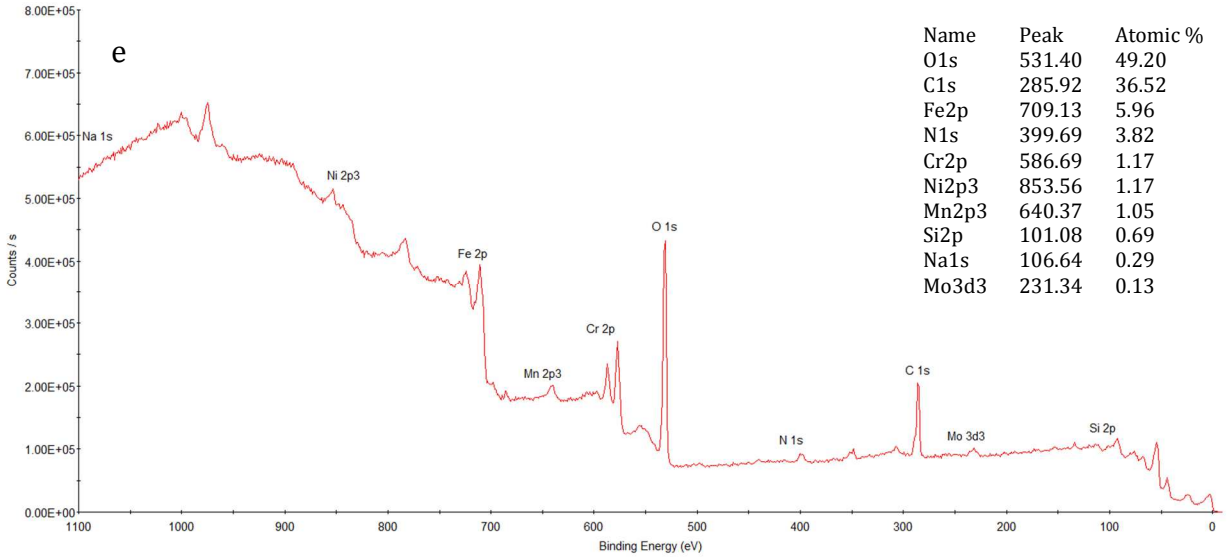

Figure 4: XPS survey analysis of 316L stainless steel: (a) UNT, (b) EPA, (c) EPB, (d) MEPA, (e) MEPB

Mentioned previously, the detection of elemental oxygen is under investigation for explicit properties capable of altering the progressive interaction with the surface oxide film layer. In a study using x-ray photoelectron spectroscopy (XPS) of the same surfaces with the four different surface treatments, a prominent detailed analysis of elemental compositions can be evaluated with exclusive relations regarding oxygen and what its potential has in forming oxides with particular elements. As XPS is a quantitative technique, which uses irradiation of a material with a concentrated beam of x-rays while instantaneously quantifying the kinetic energy and x number of electrons being removed from the bonds to reveal binding energies. Binding energies are the relative correspondents to the substantial energy required to remove or break loose these electrons from their bonds, as each element being detected has a binding energy required to remove that exact electron. The atomic percentage concentrations of elements present within the survey spectras are shown in Figure 4, which is based on the determination of peak areas. The binding energy of oxygen is at an approximation of 531 eV and Figure 4 will reveal similar

peaks in this general vicinity. What is important is the intensity at which these peaks are relevant to the atomic percentage of an inclusive scan. Figure 4a, UNT, will be the reference for the amount of elemental oxygen, oxides, hydroxides, carbonates, C – O, or C = O that may be present between the oxygen binding from the surface in the form of a surface film. Further analysis will be evaluated to better understand which chemical state oxygen may be present. Oxygen (O 1s) and carbon (C 1s) are dominant elements present on the surface throughout the four treatments, Figure 4, as the sensitivity of the XPS can divulge minute concentrations without etching through the entire surface oxide film layer. Illustrating oxygen further, the fluctuations between the atomic percentages of the treated surface can be conveyed by their respective electrochemical process.

Considering the above and below oxygen evolution for electropolishing and magnetoelectropolishing with respect to the current density plateau, it will reveal the increased formation of oxygen on the surface during the above oxygen evolution and decreased formation of oxygen on the surface during the below oxygen evolution. This theory does hold valid per XPS analysis as it shows this leading trend, however, each process of above and below oxygen evolution will have significant variances. The oxygen intensity increased for the electropolished and magnetoelectropolished above the oxygen evolution (Figure 4b, 4d) and decreased for the electropolished and magnetoelectropolished below the oxygen evolution (Figure 4c, 4e). The proficient increase of oxygen on the treated samples would indicate some oxide film layer forming on the surface, as what would be expected. This oxide can be generated with ambient air conditions as well as with more a significant approach to oxygen dissolution during the electrochemical process. Carbon, with second highest atomic percentage may be linked to the metal carbonates formed during the heated electrolyte procedure of the electrochemical process,

liberating carbon dioxide from the long and short term carbon cycle which leaves behind an oxide.

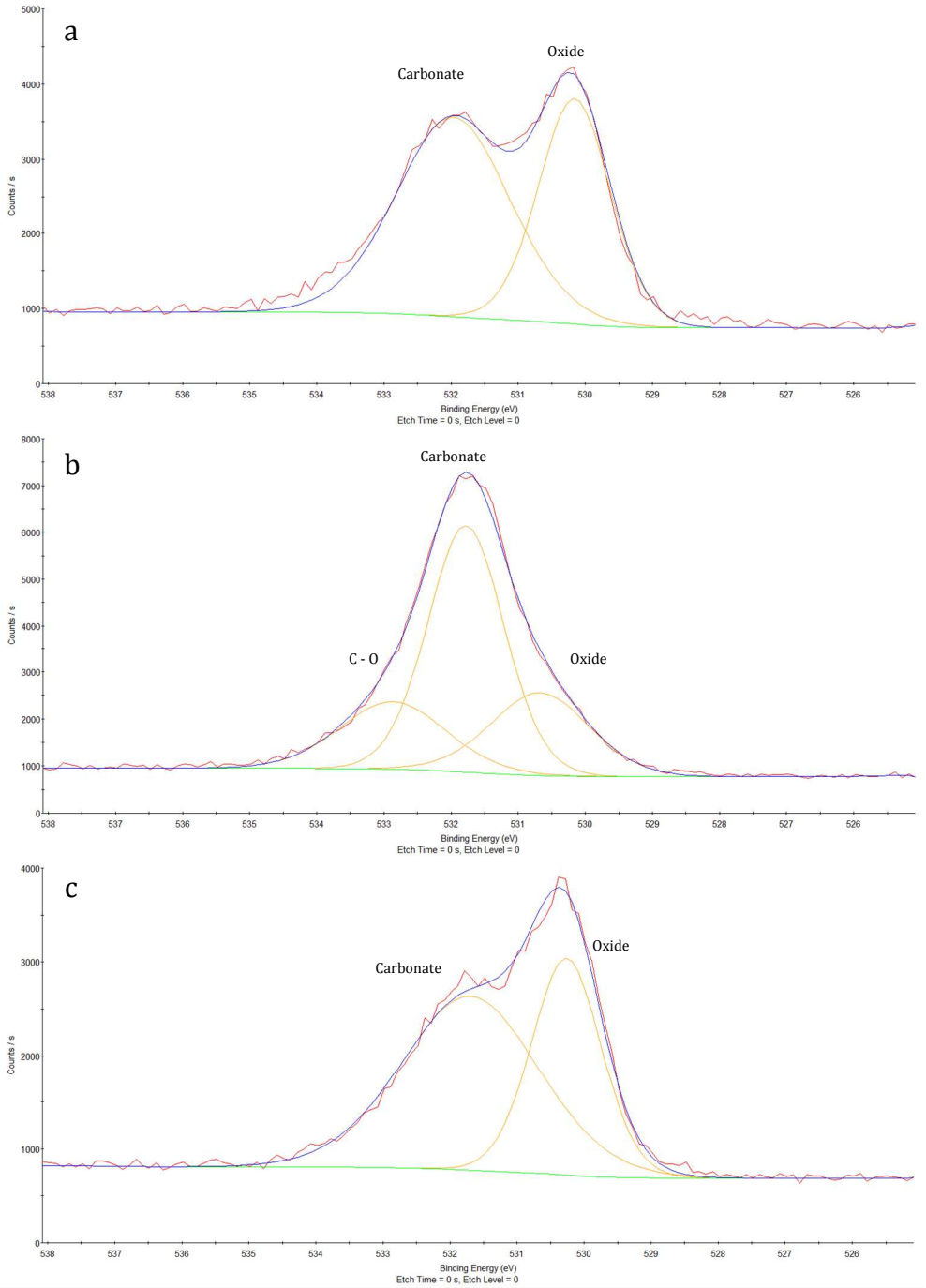

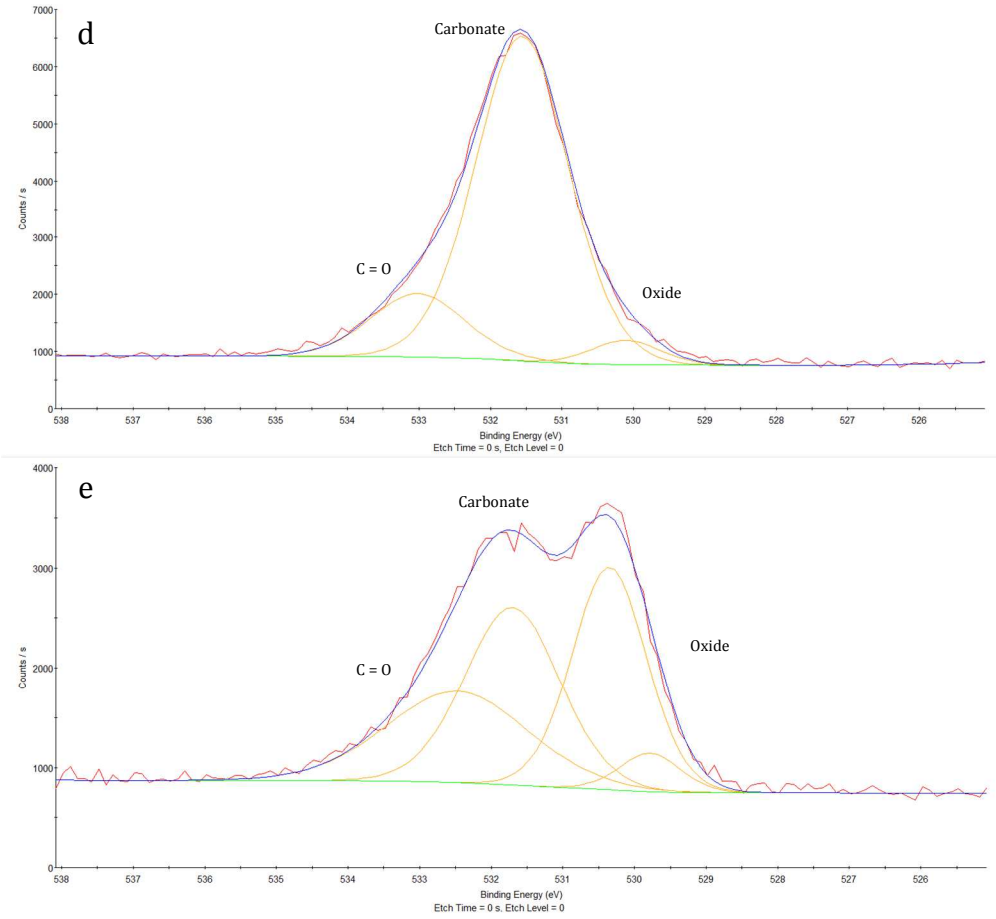

Figure 5: XPS oxygen peaking fitting analysis of 316L stainless steel: (a) UNT, (b) EPA, (c) EPB, (d) MEPA, (e) MEPB

Determining whether the increase in oxygen is relative to a protective oxide film, the chemical state binding energy of specific elements needed to create a passive layer may be observed in Figure 5. A peak fitting analysis taken from the first etched depth profile scan may reveal more to what lies within these oxygen peaks. A process of peak fitting the general overlay of oxygen, will demonstrate the ability to decisively conclude the differences of chemical bonds (i.e. C – O and C = O), carbonates, and oxides. Oxide peaks within the initial peak are present for all treatments and UNT. This is a common occurrence for passivation of the metal's surface and may be altered to favor an increased intensity with certain modifications. As mentioned beforehand, carbonates are also present in each of the treatments that will allow the outer most

layer of oxygen to be saturated but will subside while etching further in the film substrate. From these oxides, further analysis of iron, nickel, and chromium may be represented over a depth profile to quantify an approximate film thickness.

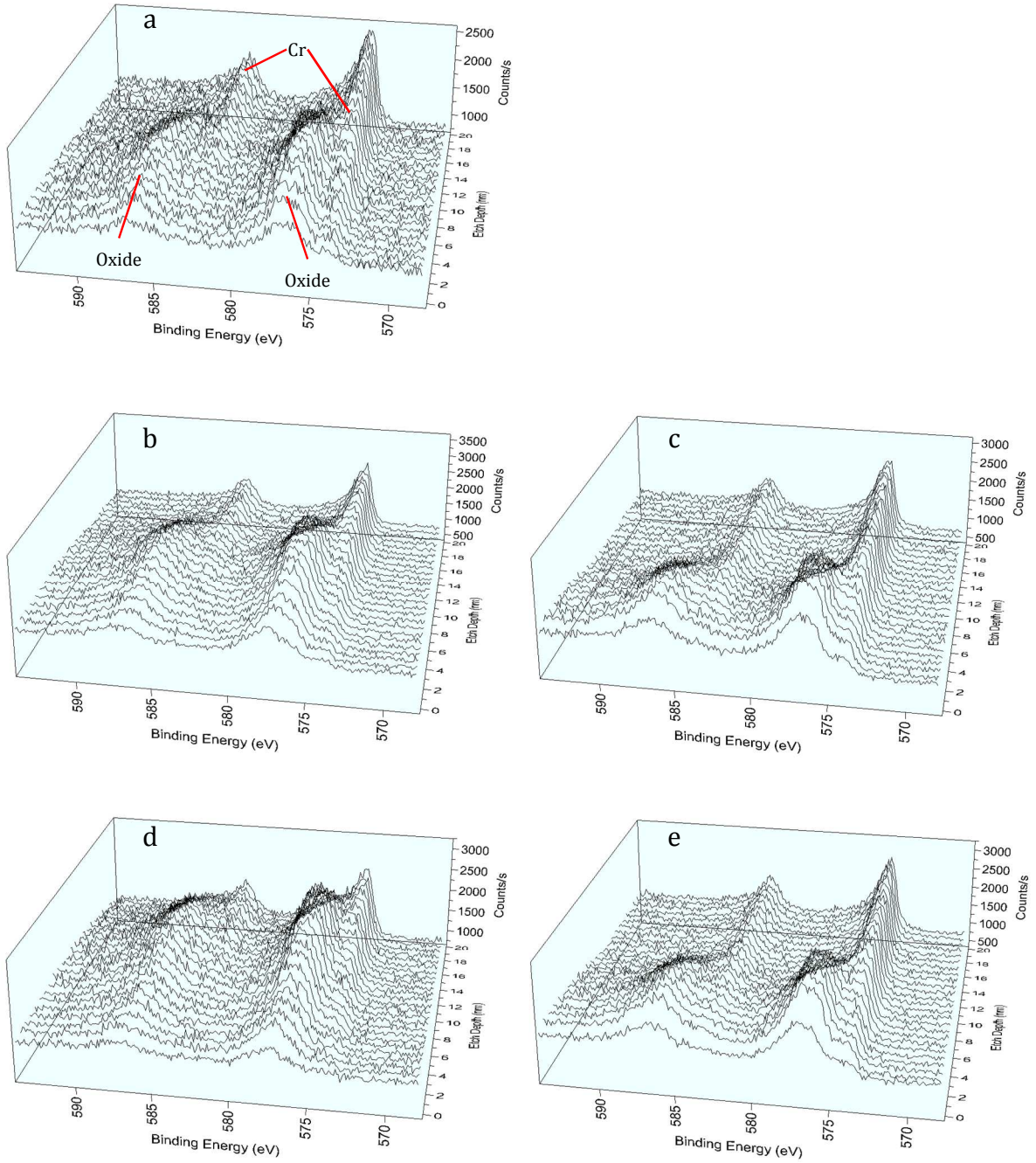

Figure 6: XPS 3-D chart analysis of Cr on 316L stainless steel: (a) UNT, (b) EPA, (c) EPB, (d) MEPA, (e) MEPB

The XPS results on the 316L stainless steel's surface for the chromium region indicate the occurrence of oxides, Cr_xO_y, in each case, with varying amount of free chromium after each consecutive electrochemical treatment of EPA, EPB, MEPA, and MEPB. After analyzing the XPS chromium region from a binding energy ranging from 568 eV to 594 eV, the metallic chromium peak is observed throughout the surface with similar binding energies for all other treatments. The chromium peaks are visible over miniscule amounts of background noise as the chromium oxides are of great interest. The sample's surface generally forms Cr_2O_3 oxides and is apparent with a binding energy of 576.5 eV. The hydroxide $Cr(OH)_3$ for chromium occurs at a binding energy of 577 eV. The occurrence of these oxides and hydroxides of chromium present on the dominant layer after electrochemical treatments would indicate a strong passive layer being created, and it is believed to be the reason for improved corrosion behavior.

Chromium has a substantial impact on the biocompatibility of 316L stainless steel, causing metallic ions to be leached into the human body, which leads to toxicity and the more progressive passive layer that can be created as an oxide film to help prevent corrosion. Chromium (III) compounds are not considered to be a health hazard, but chromium (VI) is toxic and carcinogenic. These two compounds of chromium need to be verified to as whether they are present within the oxide film after the electrochemical treatments. Based on the different profiles for the treatments, it is safe to conclude the presence of elemental chromium and chromium oxides. MEPA has a variation in the peak intensity as the etching depth increases, showing an underlining oxide film that has been created under the surface layer, which can be led to believe of an unusual formation of a chemical state reaction with chromium. Furthermore, the oxide film thickness in this region of chromium may be approximated in the 10 – 14 nm range throughout each treatment before reaching the bulk material.

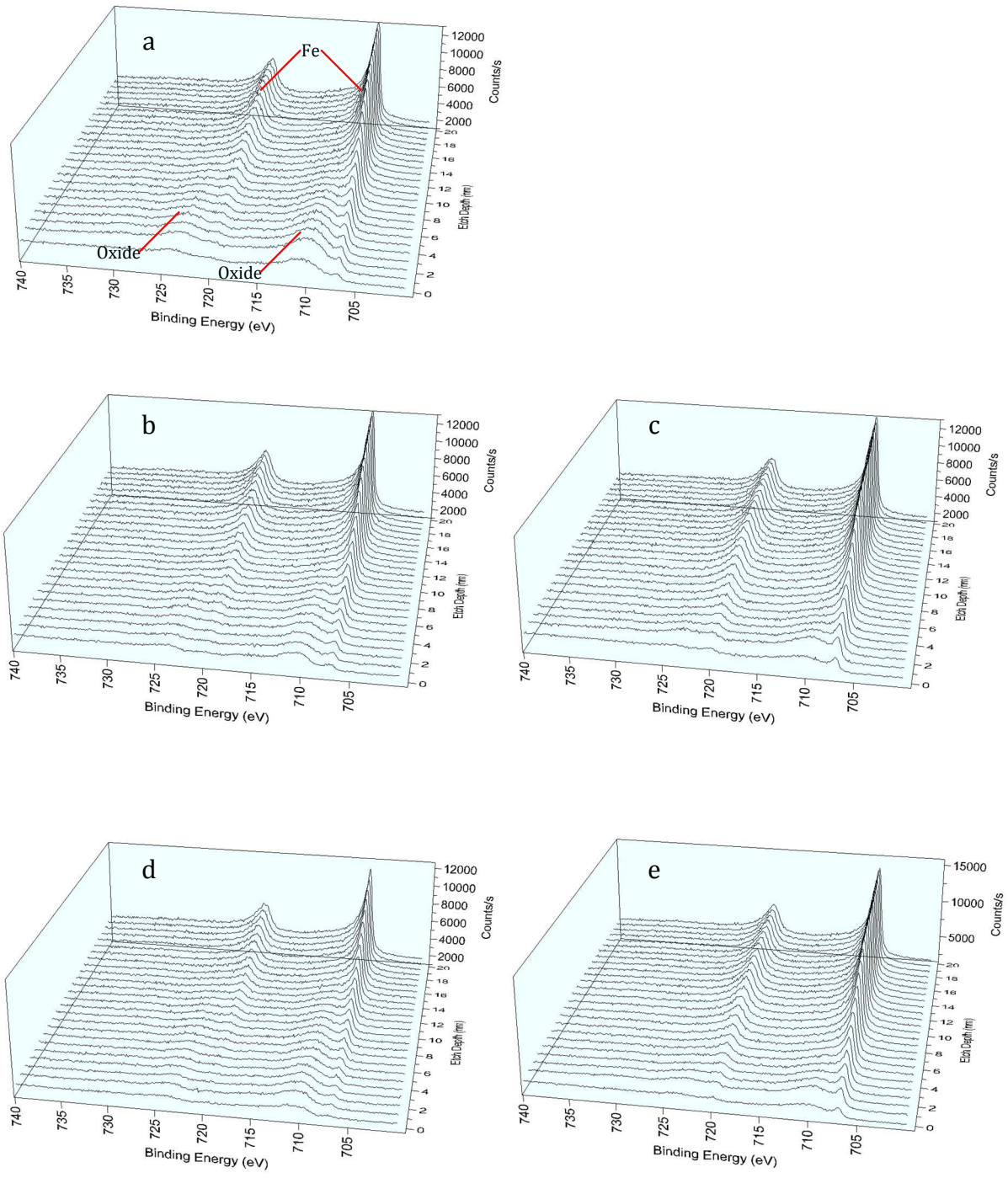

Figure 7: XPS 3-D chart analysis of Fe on 316L stainless steel: (a) UNT, (b) EPA, (c) EPB, (d) MEPA, (e) MEPB

A series of the XPS results of 316L stainless steel has been exposed with the concern of iron content. Iron has the ability to be created in the human body naturally on its own under two types of proteins: hemoglobin in the red blood cells and myoglobin in the muscle cells. If any of these two proteins are in close proximity to a 316L stainless steel implant, they could easily cause somewhat of a reaction with iron contents in the bulk properties. The toxicity of iron could cause hemochromatosis as it would be best to have very low to almost no iron levels at the surface of the sample, as shown in the 3-D high resolution spectras presented in Figure 7. The 3-D high resolution spectra displays the narrow range of a binding energy of approximately 706 eV to 710 eV for the iron, Fe 2p, 3/2 orbital region and initially indicates slight to no concentrations. However, these spectra do illustrate how the chemical state of iron (Fe) alters after each treatment's varying modification. The UNT serves as a fundamental reference for the iron (Fe) amount as the resulting treatments need to exemplify the decrease of iron and have an increased etched depth of overall oxide substrate before reaching the bulk material. The characteristic features have significant differences in iron (Fe) contents between each surface treatment. Iron does not show a strong oxide area as compared to that of chromium and this does demonstrate the potential of iron ions to be released as the film thickness is in the approximate range of 4 – 6 nm before reaching the iron bulk material.

Further, study was carried out on the Fe 2p peaks to reveal the two orbitals of oxygen formation with electrons. The peaks of Fe $2p_{3/2}$ and Fe $2p_{1/2}$ are shown in Figure 7. Of the two peaks the Fe $2p_{3/2}$ peak is narrower with a stronger intensity and greater peak area than that of the Fe $2p_{1/2}$ and the area of Fe $2p_{3/2}$ peak. The peak position of Fe $2p_{3/2}$ is approximately at 712 eV, between other researchers the position may range between 710-713 eV, and the region has visual associated satellite peaks. The binding energies of Fe $2p_{3/2}$ and Fe $2p_{1/2}$ obtained from the present

study are 711.0 eV and 724.6 eV, respectively. The satellite peak obtained at 718.8 eV is clearly distinguishable and does not overlap either the Fe $2p_{3/2}$ or Fe $2p_{1/2}$ peaks. In addition, there appears to be another satellite peak at 729.5 eV; this may be a satellite peak for Fe $2p_{1/2}$.

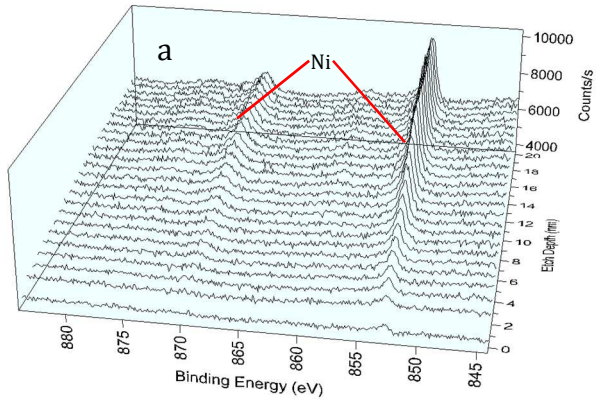

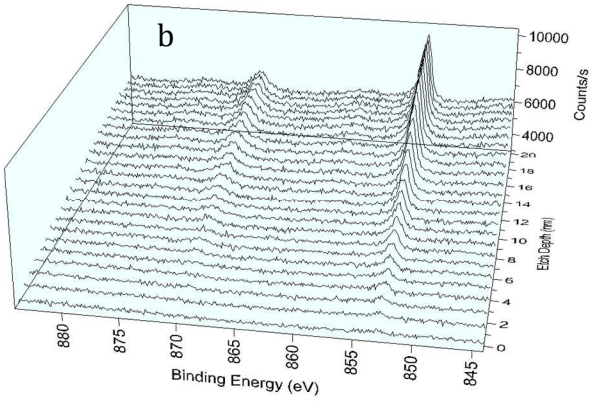

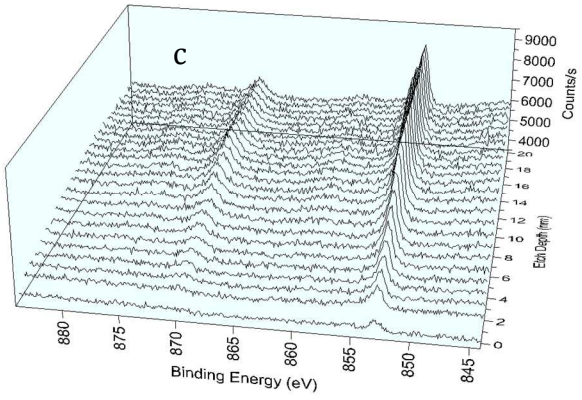

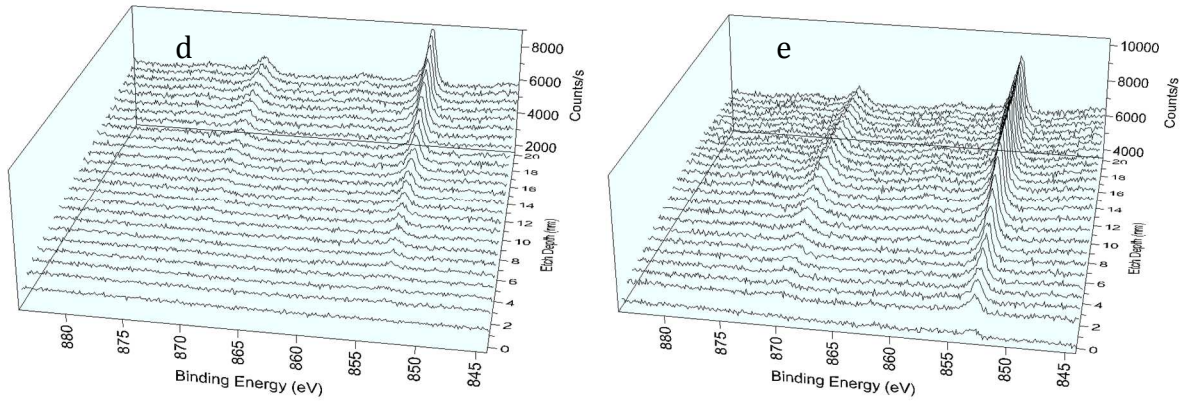

Figure 8: XPS 3-D chart analysis of Ni on 316L stainless steel: (a) UNT, (b) EPA, (c) EPB, (d) MEPA, (e) MEPB

Thus, leading to the final analysis performed over the alloying elements, nickel has shown that oxidation from the electrochemical process ultimately removes formation of any oxide layer containing nickel on the first etched scan. This process, whether for the UNT or for each treated surface is an exemplary example to achieve the preventions of nickel ions being released. Its film thickness and composition varies throughout the samples and can convey to an approximation of 10 nm, with a sputter rate of 0.17 nm/sec referenced to a SiO_2 wafer, film layer before being able to etch into the bulk properties for MEPA and the remaining treatments to depend on the electrochemical process. The nickel (Ni 2p) in the 3/2 orbital spectrum exhibits an elemental concentration that becomes increasing intensified over time and would indicate reaching majority of the bulk material.

XPS analysis was carried out on the Ni 2p peaks. The peaks of Ni $2p_{3/2}$ and Ni $2p_{1/2}$ are shown in Figure 8, of the two peaks the Ni $2p_{3/2}$ peak is narrower with a stronger intensity and greater peak area than that of Ni $2p_{1/2}$ peak. The peak position of Ni $2p_{3/2}$ is approximately 852 eV, among other researchers may range between 851-853 eV, and has associated satellite peaks as the etch depth increases. The binding energies of Ni $2p_{3/2}$ and Ni $2p_{1/2}$ obtained from the

present study are 852 and 870 eV, respectively. The formation of oxide is only applicable after the increase of elemental nickel, and as the presence increases, the chemical reactions initiate the bonds to form a minor oxide regime further on.

Surface Roughness

The integration of a biomaterial's surface is relative to the interaction between the material and the living tissue, factors that contribute to the success or failure of an implant is the surface topography and surface free energy [112]. The surface interaction the material has great influence on MC3T3 pre-osteoblast and human umbilical vein endothelial cells. With implants being incorporated into the bone in hip implants, the material's surface needs to have the ability to support osseointegration, and in coronary stents it is essential that the endothelial cells regenerate inside the inner lining of the artery wall. Osseointegration is the connection between the implant and remodeling of bone without the presence of soft tissue at the microscopic level [113]. The micro scale surface roughness is influential for permanent implants for the long term biomechanical integrity of the interface between the bone and implant due to the greater surface area. The rougher the surface the more positive of an impact on the osseointegration, exceptional cell adhesion and improved biomechanical interaction [114]. Although, increased roughness causes corrosion susceptibility and initiates pitting in its oxide layer [115].

The atomic force microscope (AFM) surface topography of each treated sample is shown in Figure 9. The electrochemical treatments, whether being EPA and MEPA being above the current density plateau or EPB and MEPB being below the current density plateau with either an increased or decreased amount of oxygen removing ions will convey toward a roughness between which inclusions and surface area are a considering factor for corrosion and biocompatibility. Similarly, as the increase of oxygen occurred for the XPS analysis showing an

increased atomic percentage of oxygen concentration; a similar effect will occur for the roughness aspect as the increase of oxygen dissolution of ions from the surface at varying rates is dependable on electrochemical treatment itself. The roughness can be contributed to a lower dissolution rate with the expenditure of more oxygen, as there will be larger deviations of peaks and valleys considered to be increased inclusions of the surface. Equally, with a higher dissolution rate with the decreased presence of oxygen, as there will be smaller deviations of peaks and valleys considered to be decreased inclusions. These inclusions may have a positive or adverse affect at which they may help with increasing the surface area for cell adhesion, but will also affect the area exposed to harmful fluids that may increase the corrosion rate. As the roughness is associated with the peak to peak amplitude over a given wave period (i.e. sinusoidal wave), the peak height or amplitude is a factor of determining the ability to successfully obtain cellular adhesion while sufficiently reducing the effects of pitting corrosion.

Figure 10 is the data yielded from the AFM as a comparative analysis bar graph of the average roughness, Ra, for each treatment modification. The EPA and MEPA yield the higher roughness while the EPB and MEPB produced the lower roughness, even below the UNT. The highest roughness is MEPA with 11.8354 nm and the lowest being MEPB 8.8154 nm, the reason for the roughness being under the category of magnetoelectropolishing as opposed to electropolishing may be due to the different parameters used during the electrochemical process. Table 7 represents the average and root mean squared roughness obtained from the AFM scanned readings. The results indicate that the below oxygen evolution for the EPB and MEPB samples show a relatively substantial difference in roughness compared to that of the UNT. Although, considering the increase and decrease of the micro roughness, the overall surface area in turn may lead to proficiency in cell adhesion and attachment for proliferation. Optimal

mechanical interlocking of implant and optimum surface roughness to the host tissue is required to achieve acceptable integration of implant and tissue.

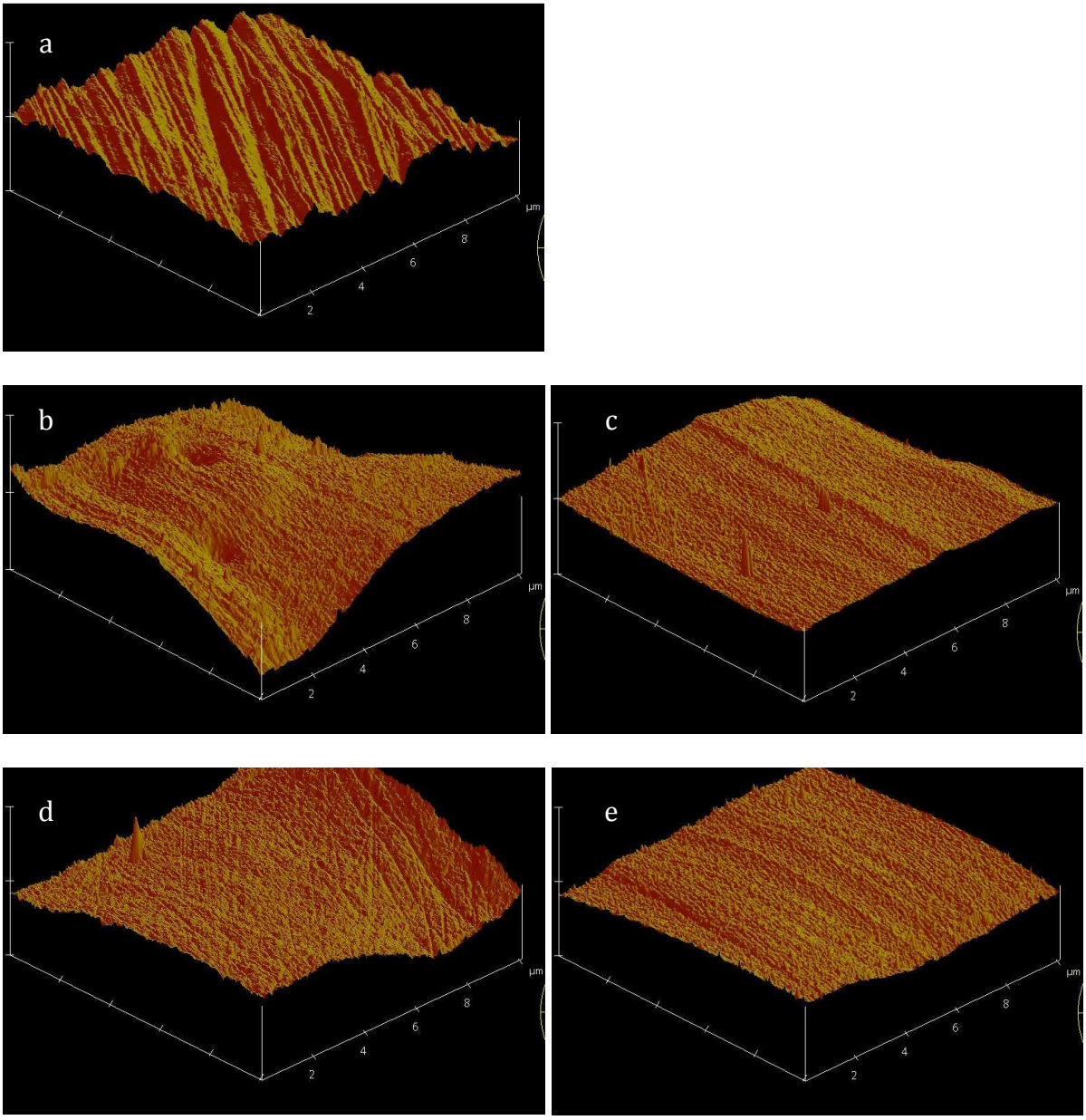

Figure 9: AFM of 316L stainless steel: (a) UNT, (b) EPA, (c) EPB, (d) MEPA, (e) MEPB

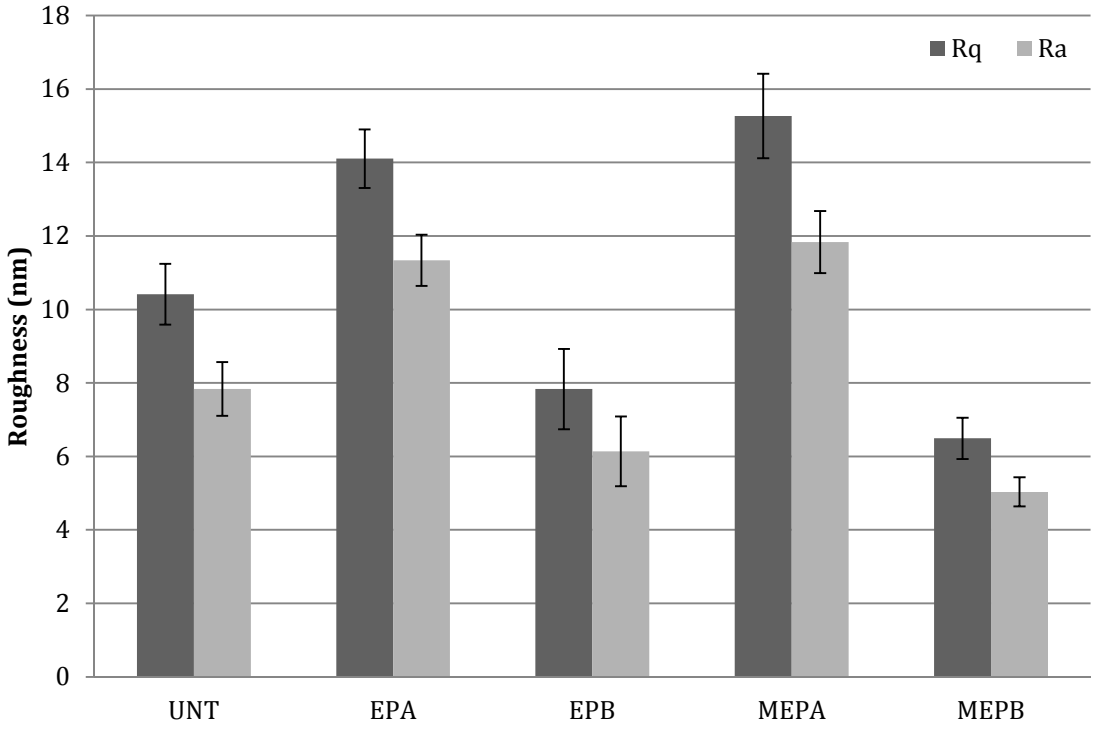

Figure 10: AFM roughness of 316L stainless steel

Table 7: AFM roughness of 316L stainless steel

	Root Mean Square Rq (nm)	Avg. Roughness Ra (nm)	Avg. Max Height Rpm (nm)	Avg. Max Depth Rvm (nm)
UNT	10.4142	7.8354	13.0652	-12.6336
EPA	14.1054	11.3362	16.612	-15.7394
EPB	7.8314	6.1378	10.6528	-8.654
MEPA	15.2656	11.8354	17.4416	-17.197
MEPB	6.491	5.0334	8.8154	-7.5268

Wettability

In the case of all the 316L stainless steel treatments, the contact angle exhibits significant difference after the surface chemistry has changed the characteristics necessary for hydrophilicity or hydrophobicity due to surface oxygen content. The oxygen content alters the dipole movement of the water droplet on the surface substrate, affecting the molecule's orientation and thus the droplets behavior on the surface. The wettability in Figure 11, 12, and 13 show a significant decrease in the contact angle among all the treatments proposed amid three different testing fluids consisting of dionized H_2O (mildly polar), ethyleneglycol (neutral), and diiodomethane (highly polar). The data was taken from ten readings per solvent on each of the treated samples at locations separated by sufficient spacing in order to prevent any previous obscurities from the droplets. FAMAS analysis software was utilized to calculate the contact angle, surface free energy, interfacial free energy, and work of adhesion on the coupons by employing two theories of acid-base and kitazati-hata. The interaction of water and proteins on the biological interface occurs from the inversely proportionality of surface free energy to the contact angle [116]. Cell proliferation and biocompatibility is enhanced with moderate hydrophilic properties as compared to that of super hydrophilic surfaces [117].

This investigation entails the contact angle to lean toward a hydrophilic ($\theta < 90°$) surface for the four surface treatments and decreased over the three solvent fluids. Hydrophilicity permits higher osseointegration and a more mechanically stable structure. The benefit of a hydrophilic surface is having a better general cell adhesion to be more stable than a hydrophobic surface. The surface oxide layer has some influence on the polar bonds that dictate the droplets interaction with water and proteins (amino acids). The mean values of surface free energy would indicate that the UNT having the highest surface free energy and EPB having the lowest for all

solvent fluids. The surface free energy has an influence on cell proliferation and lower values signify more proficient cell activity, as thrombogenicity increases with increased surface free energy. Lowering the surface free energy corresponds to favorable cell adhesion and activity. In this case the surface free energy is just beyond the ideal cell activity range, but does not mean these treatments are not favorable for cell adhesion. Table 8 and Figures 11, 12, and 13 summarize the resultant measurements of the contact angle, work of adhesion, and surface free energy.

The work of adhesion for the different polarized solutions is interrelated to the contact angle and surface free energy and vise versa intended for dissimilar particles to cling to one another. The particles between the cells and materials surface need to be increased, as the cohesion will exemplify the need to cohere. The surface free energy may be explained with the disorder of intermolecular bonds as the treatments altered the surface; the molecules on the surface have a higher surface free energy compared to the materials bulk free energy. Another reason for using three different solutions is the energy density and surface tension adversely affecting the wettability of each treatment. The results illustrate the properties of strong adhesion and weak cohesion with a low contact angle and high wetting.

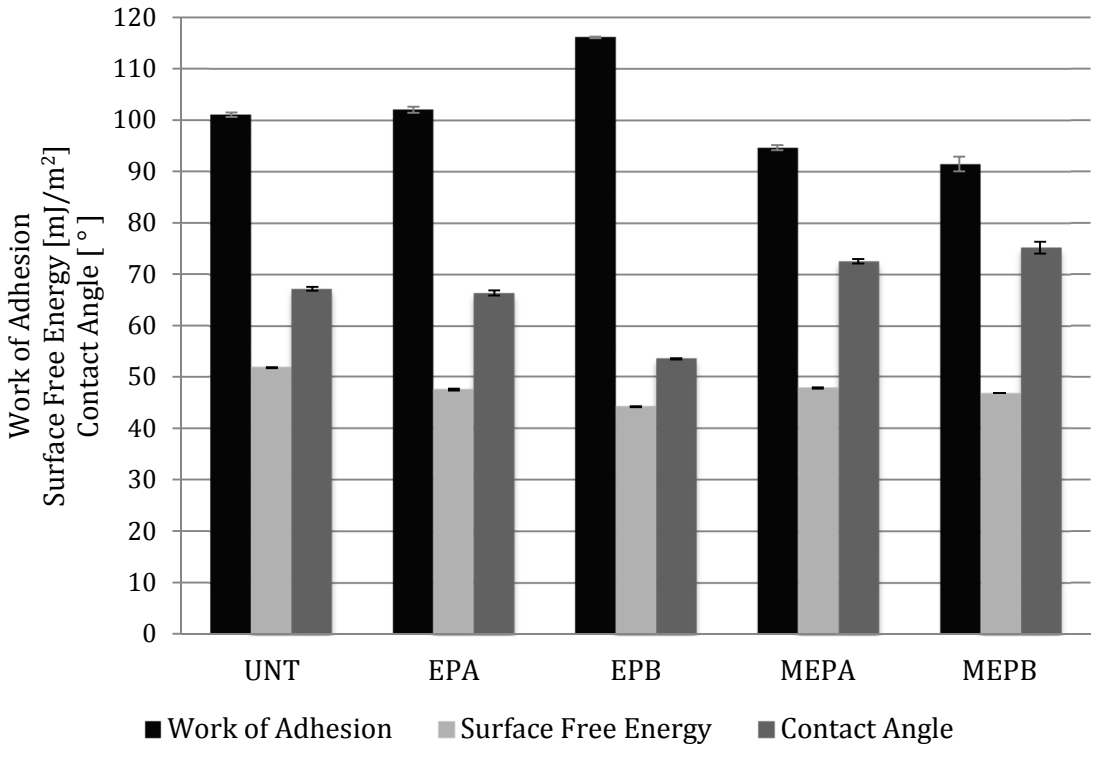

Figure 11: Acid-Base (DI H_2O) surface values of 316L stainless steel

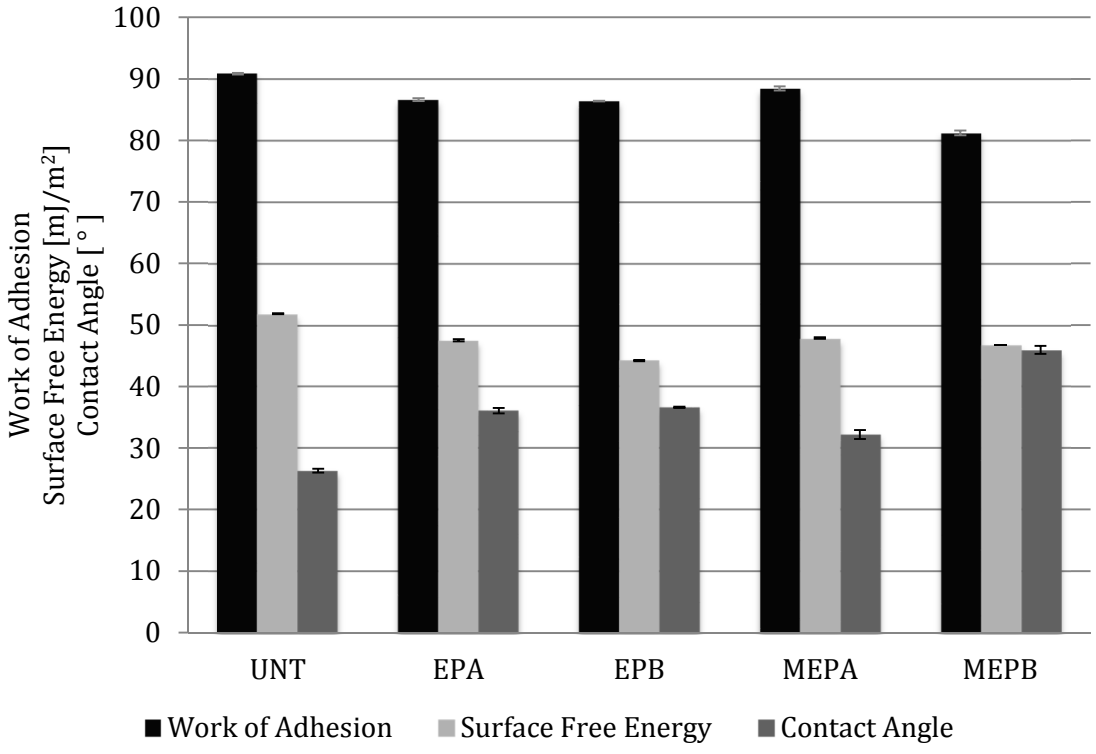

Figure 12: Acid-Base (ethylene glycol) surface values of 316L stainless steel

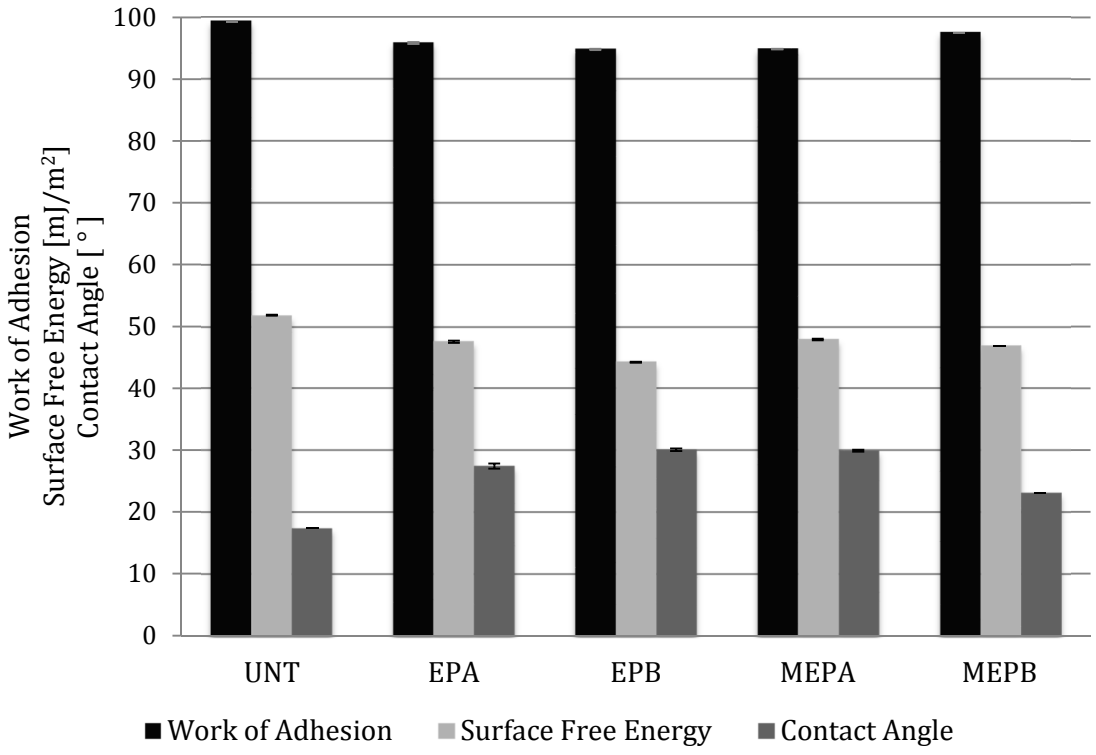

Figure 13: Acid-Base (diiodomethane) surface values of 316L stainless steel

Table 8: Wettability data of 316L stainless steel

Acid – Base	Contact Angle (°)			Surface Free Energy (nJ/m^2)			Work of Adhesion (nJ/m^2)		
	DI H_2O	Ethylene-glycol	Diiodo-methane	DI H_2O	Ethylen-eglycol	Diiodo-methane	DI H_2O	Ethylene-glycol	Diiodo-methane
UNT	67.16	26.3	17.4	51.81	51.81	51.81	101.06	90.84	99.3
EPA	66.35	36.07	27.43	47.52	47.52	47.52	102.01	86.61	95.85
EPB	53.51	36.63	30.04	44.21	44.21	44.21	116.09	86.37	94.81
MEPA	72.54	32.21	29.92	47.86	47.86	47.86	94.63	88.43	94.86
MEPB	75.17	45.96	23.1	46.8	46.8	46.8	91.44	81.21	97.5

Cyclic Potentiodynamic Polarization

A phosphate buffer saline (PBS) was used to simulate internal human body fluid as the solution has the same chemical composition with a process to decrease the concentration of dissolved oxygen and to achieve a de-aerated environment for corrosion analysis. The extracted

corrosion data was then plotted with current density in A/cm^2 on the x-axis using a logarithmic scale versus potential in V on the y-axis.

The method that the cyclic potentiodynamic polarization undergoes occurs by a technique involving a forward and reverse polarization. This is a technique implicating the potential of an assessment controlled by the corrosion current, which is measured by a potentiostat to quantify the electrochemical resistance. A supporting theory leads the cathodic curve representing hydrogen evolution through a reduction process and the anodic curve signifying the oxidation. This process of measuring the electrochemical resistance is similar in method as to how the electrochemical treatment mechanism is equivalent to anodic leveling or removal. The potential is scanned in a forward (noble) direction and continued until reaching a specific or predetermined current density. Once the transpassive region is reached, no longer demonstrating passivity, the scan is then reversed until the sample reaches a repassivation phase. This is a beneficial method for determining the metals susceptibility to pitting while in a corrosive environment and these measurements were used to asses the active passive characteristics of the UNT and four surface treatments. After, the Tafel fit and Tafel extrapolation method was implemented to evaluate the polarization curves where the passivation occurs by selecting multiple points ±30 mV starting from the E_{corr} values across each treatment.

There was no observed hysteresis loop during the repassivation phase of the polarization scan and all the scans followed the general feature of active, passive, and transpassive regions shown in Figure 14. The cyclic polarization curves are evaluated by the formation and loop area to determine the general pitting and crevice corrosion. The increased loop area the greater the inclination to pitting and crevice corrosion the material will experience. The reverse scans taken from the subjected treatments take an alternative path trajectory, an exceptional trait toward the

resistance of corrosion. An outcome from the results gained would lead to believe the treatments yielded a decreased loop area and a slightly dissimilar reverse scan, promoting more corrosion resistance to that of the UNT.

The 316L stainless steel alloy with the treatments under corrosion are shown in Table 9 and the maximum corrosion rate of EPA was observed. Although, the treatments have shown a progressive decrease in current density as opposed to the UNT. A decrease in this current density of MEPA with $15e^{-9}$ A/cm^2, Table 9, promotes the improvement in determining the corrosion rate as this is an important characteristic. Another considerable characteristic to increase corrosion resistance would be the increase of potential to experience a more noble behavior in the region. With EPA having the higher potential and lower current density, the overall characteristic factors of MEPA has the superior corrosion resistance to pitting and crevice corrosion with the lowest corrosion rate of $6.047e^{-3}$ mV. Also, the E_{corr} and I_{corr} values from the reverse scan shows a trend of being above the initial forward scan of E_{corr} and I_{corr} for some of the treatments, indicating an increased passivation.

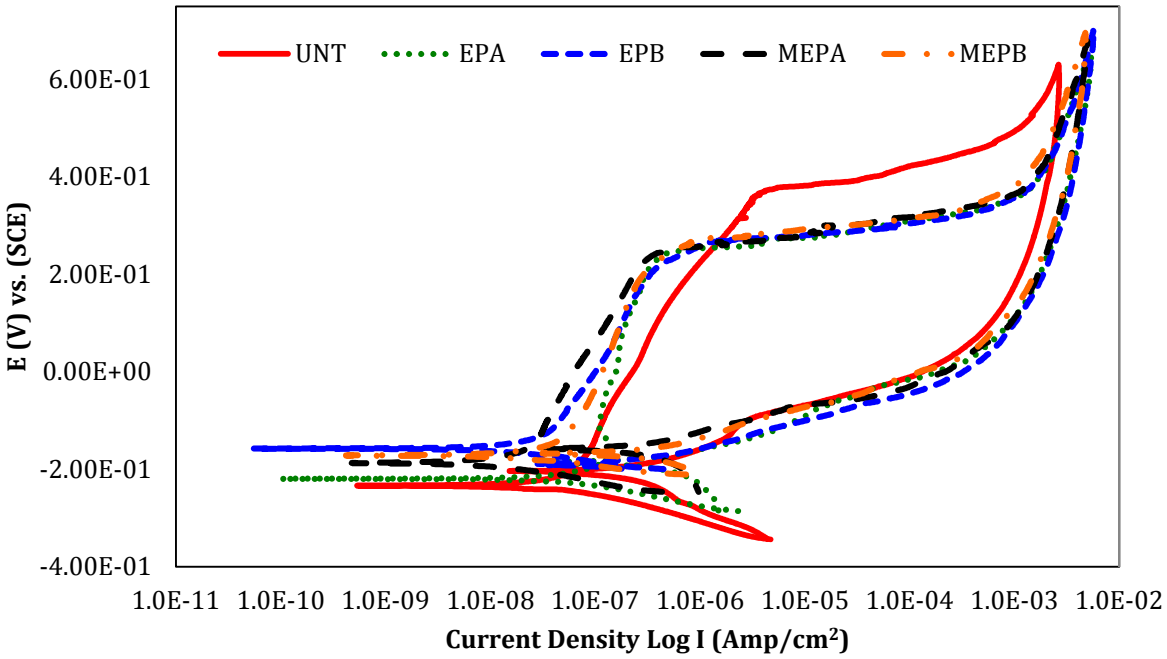

Figure 14: Cyclic potentiodynamic polarization scans

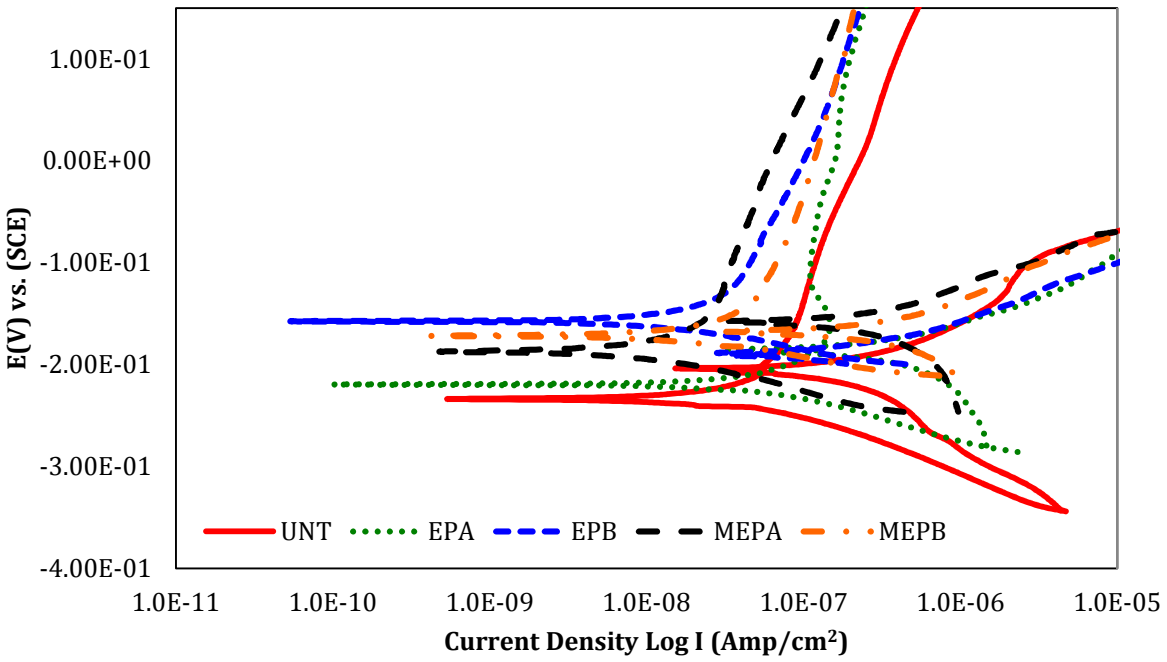

Figure 15: Enlarged cyclic potentiodynamic polarization scans

Table 9: E_{corr} & I_{corr} of electrochemically surface treated 316L stainless steel

	UNT	EPA	EPB	MEPA	MEPB
Icorr (A/cm^2)	118.0e-9	135.0e-9	18.10e-9	15.00e-9	23.30e-9
Ecorr (mV)	-234.0	-219.0	-157.0	-187.0	-172.0
Corrosion Rate (mpy)	47.43e-3	54.52e-3	7.287e-3	6.047e-3	9.407e-3

Cell Toxicity

In this investigation, the survival effects of both pre-osteoblast and human umbilical vein endothelial cells will be analyzed after metallic ionized media was released from 316L stainless steel under the assessment of an immersion test before acquiring the data from the MTS assay. The values of absorbance were converted into a comparative line graph as shown in Figure 16 and 17. The cell viability decreases over the course of increasing amount of days to which indications of toxic effects from metallic ions from the immersion test.

The cell viability was studied with a 100% concentration of extracted ionized media and Figures 16 and 17 exhibit this cell viability versus time exposure. With the use of the 100% concentrated ionized media, the general trend of viable cells will decrease over time as the leaching of ions increase over the time spent with media in contact with the sample. The results for both experiments indicate the negative effects the ionized media has on cell proliferation. As the increased ion progressed over the submersion day cycle, the cell survival decreased. From the initial day 3 to the final day 12 of the experiment, majority of the studies yielded a decrease in cell survival for each treatment. The few discrepancies as in Figure 16, EPB having a sudden increase in cell survival on the 12 day may have a multitude of varying factors. In this case, the approximation of seeding 20,000 cells in the single well may have been more due to an instrumentation error, the homogenizing of the concentration of ionized media, or the repassivation of the oxide surface to reduce the exchange of released ions. The same could be

held accountable for Figure 17 as the UNT began an immediate recovery to surpass the treated samples with a higher cell survival.

Overtime, the rate at which the ratio of viable cells are evaluated from the treatments need to be within a respectable range to formulate a positive response as a biomedical solution. The MEPA and EPB treatments showed progressive resilience to cytotoxic effects from the released ions over the 12 day span and show an overall cell survival rate more than the other treatments for the pre-osteoblast cells. However, the trending results for the human umbilical vein endothelial cells showed a steady phase of cell proliferation for EPA and MEPA.

The cell viability behavioral trend of MEPA was less cytotoxic to the pre-osteoblast and human umbilical vein endothelial cells than any other treatment. The results would also indicate that the cell viability for majority of the treatments was greater than 70%, which would suggest that of cytocompatibility. The net cell growth on average for both studies signify cell proliferation and cell survival to be substantial to consider these treatments viable from the plotted data.

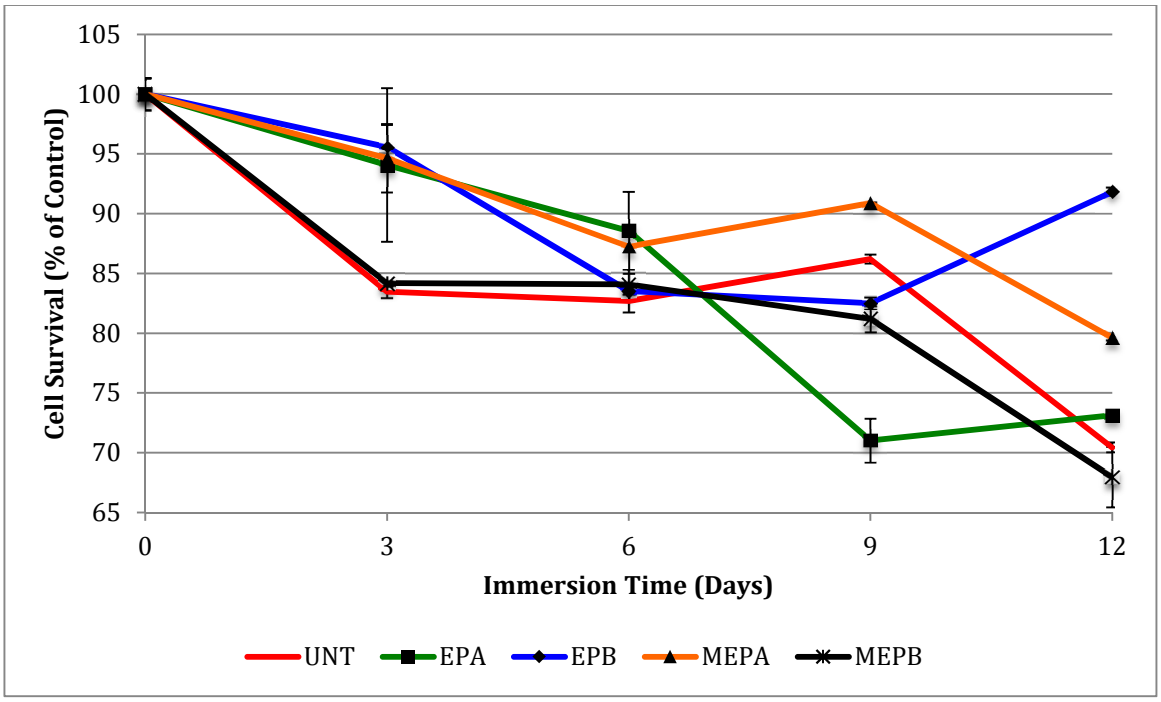

Figure 16: MTS assay of pre-osteoblast cells on 316L stainless steel

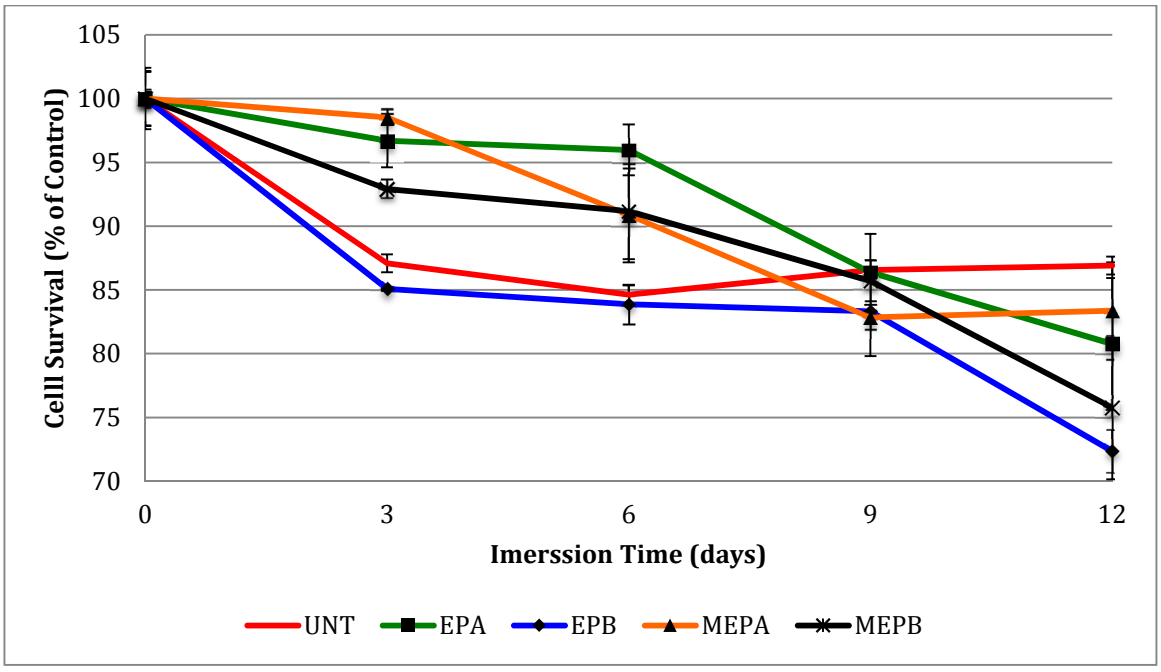

Figure 17: MTS assay of human umbilical vein endothelial cells on 316L stainless steel

Direct Cell Viability

The ability of a cell that originates from the surrounding environment within a tissue or cell to populate with intercellular signaling needs to be determined. Mimicking the natural tissue healing environment and optimizing components for an engineered material as a bone substitute, the importance of endogenous signaling profiles between cell populations needs to be taken into consideration consideration [118]. This signaling profile amongst cell population is interlinked with cell density that relates to proximity to cellular distance. Cell density is a critical parameter in controlling subsequent cell proliferation and can alter the cell-cell distance in paracrine signaling [118]. The cell attachment and proliferation of human umbilical vein endothelial cells are defined by the short term interactions and integration [119]. Therefore, the growth of cell lines on a surface is defined by their initial attachment behavior [120].

In an approach to the fixation of seeded cells for an incubation period of 3 days has led to cell adhesion and growth in cell proliferation of the treatments. These results indicate the initial adhesion of the cellular structure and matrix of the pre-osteoblast cells and human umbilical vein endothelial cells. The treatments offer a higher cell adhesion interaction with corresponding cell density. The treatments in Figure 18 and 19 produce a surface capable of promoting cellular proliferation in their immediate environment, which shall increase the viability of these modified surfaces. This study would suggest cell survival for the surface treatments to be correlated and associated with successful biocompatibility to further improve osseointegration and endothelialization. Further study of fluorescence microscopy would relate cellular process, such as spreading, proliferation, and differentiation in connection with development between the healthy cell structure composed of a nuclei and mitochondria.

The configuration in the fluorescence microscopy study of pre-osteoblast and human

umbilical vein endothelial cells was analyzed by staining nuclei in a blue color and mitochondria in a red color as shown in Figure 20 and 21. The intracellular matrix is visible with the interactions amongst each of the cells close proximity and proliferation. The cellular structure is proficient in the cell proliferation among each treatment compared to the UNT sample. The results of each treatment would lead to more profound cell proliferation with a greater confluency while showing increased signaling and connective linkage. The conditional health of the cells may be determined by the structural formation of their long bodied extrusions in multiple directions to promote cell viability, interaction, and adhesion.

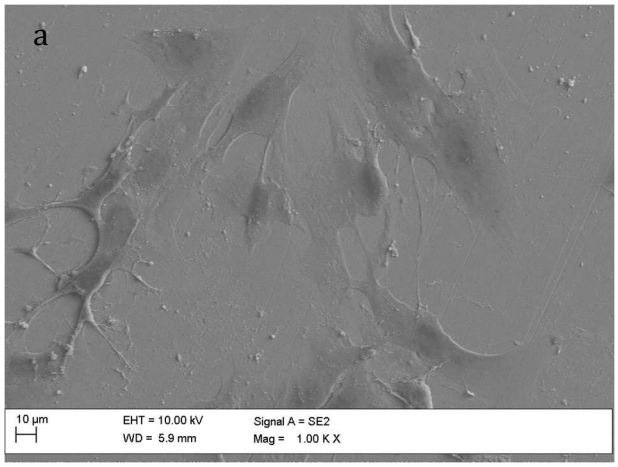

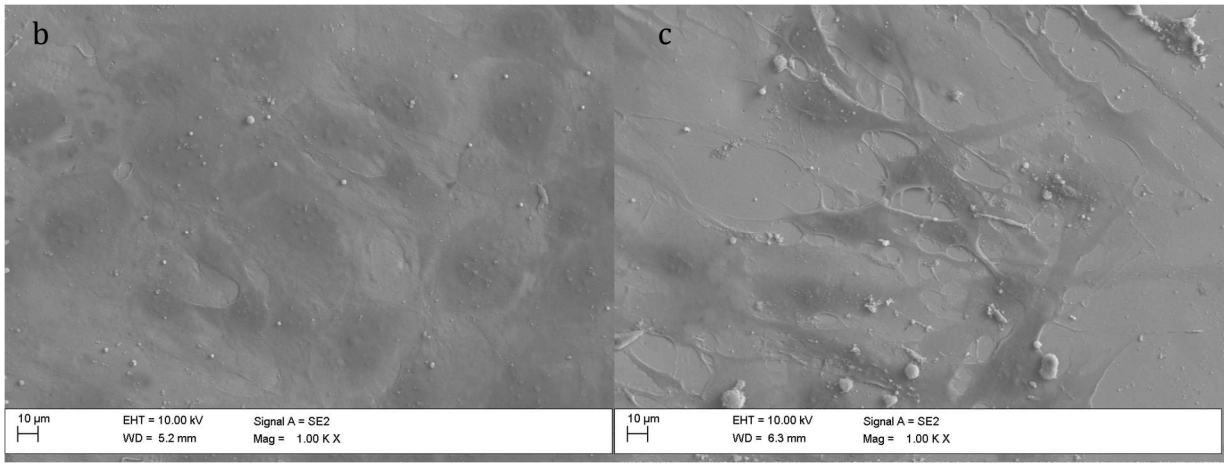

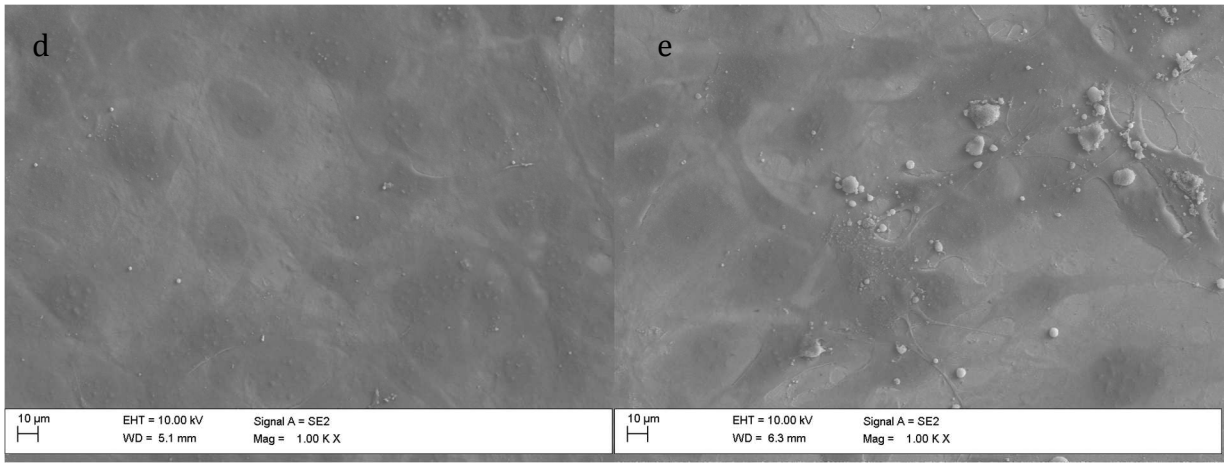

Figure 18: Pre-osteoblast cell fixation: (a) UNT, (b) EPA, (c) EPB, (d) MEPA, (e) MEPB

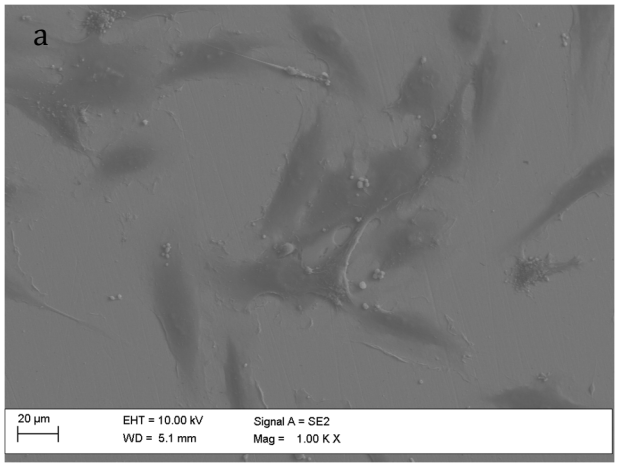

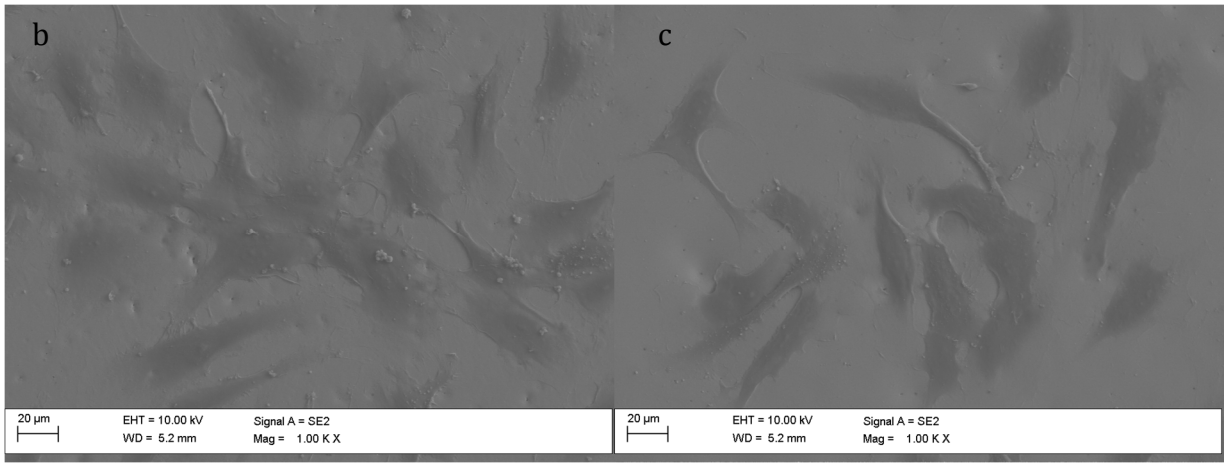

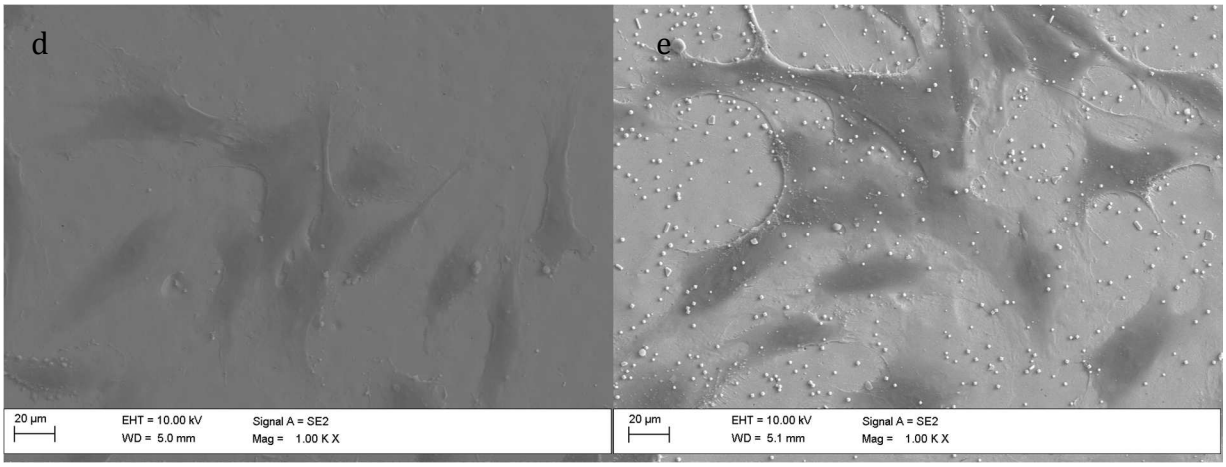

Figure 19: Human umbilical vein endothelial cell fixation: (a) UNT, (b) EPA, (c) EPB, (d) MEPA, (e) MEPB

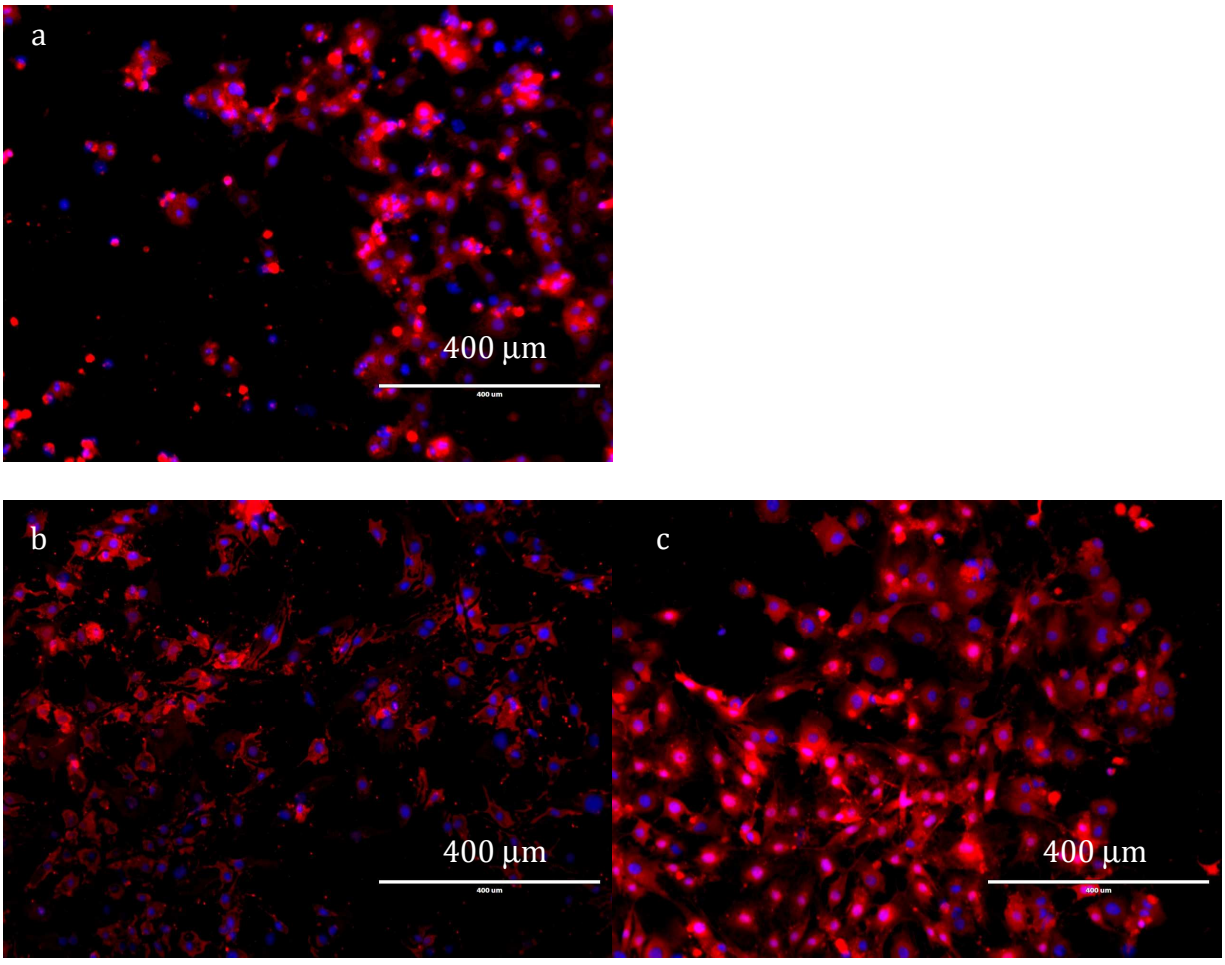

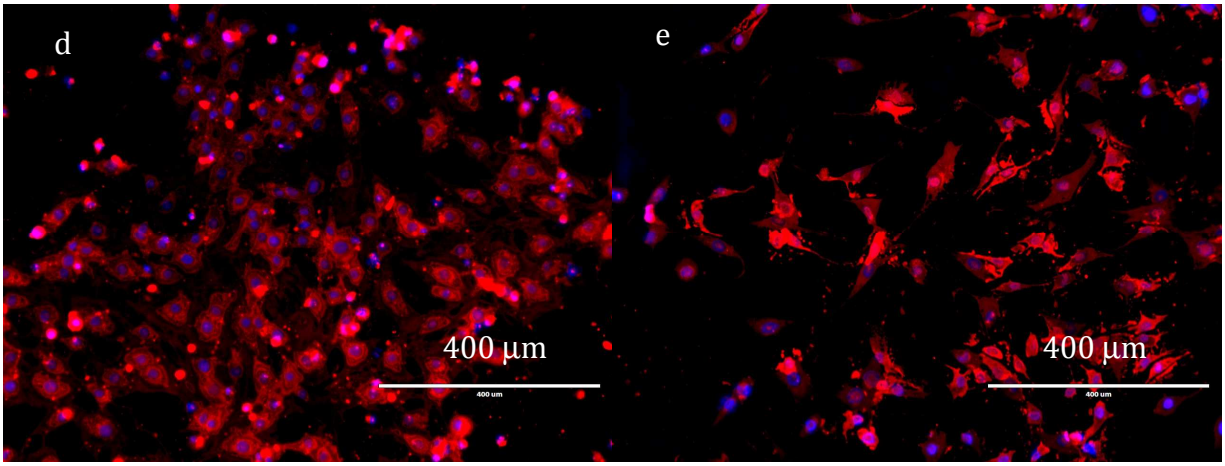

Figure 20: Pre-osteoblast cell staining of nuclei and mitochondria: (a) UNT, (b) EPA, (c) EPB, (d) MEPA, (e) MEPB

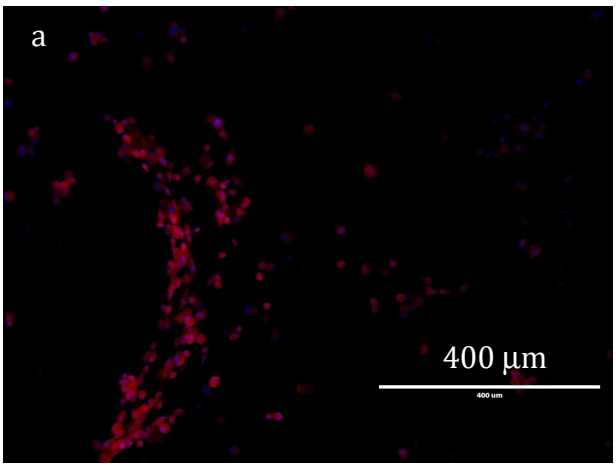

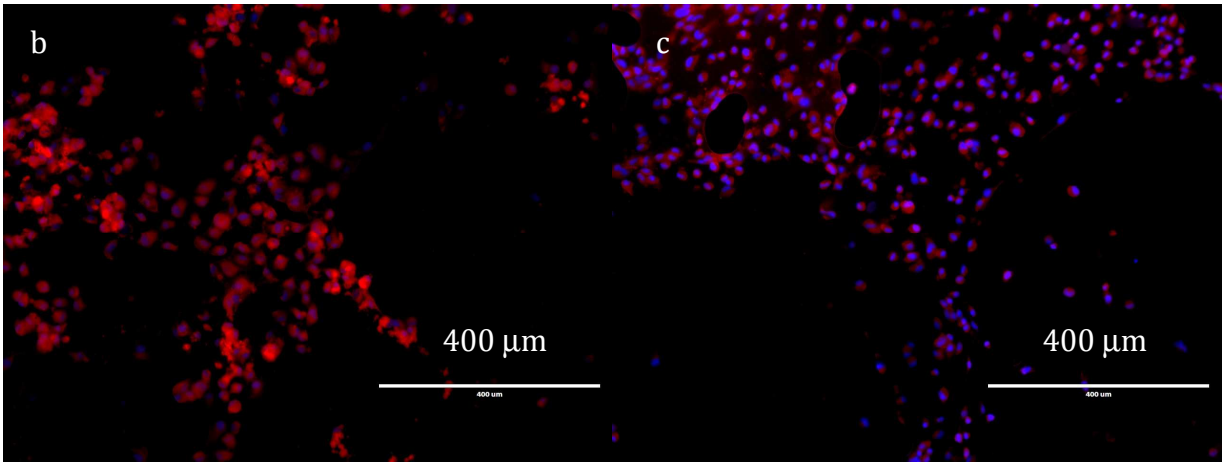

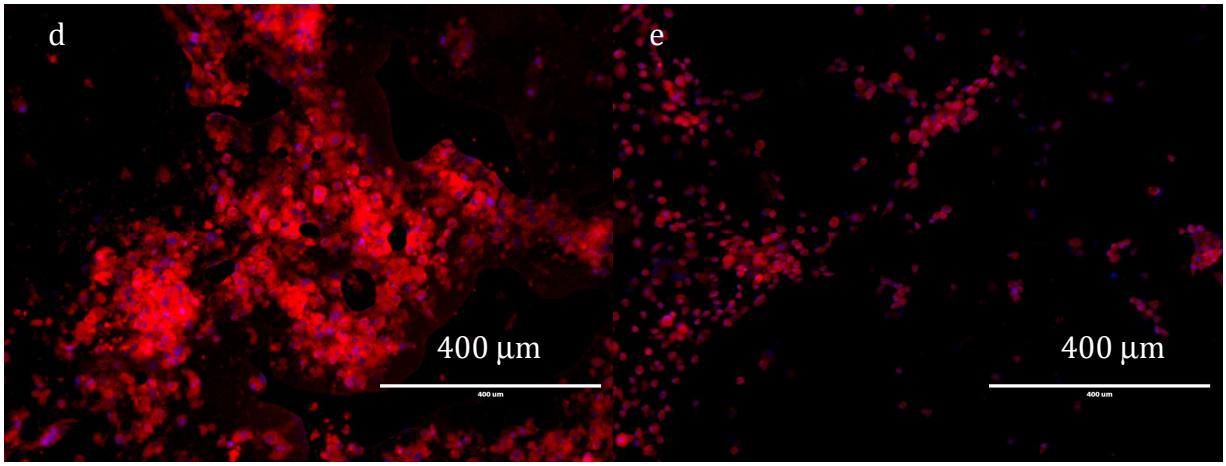

Figure 21: Human umbilical vein endothelial cell staining of nuclei and mitochondria: (a) UNT, (b) EPA, (c) EPB, (d) MEPA, (e) MEPB

CHAPTER V

CONCLUSION

The purpose of this study was intended to find an alternative technique to achieve enhanced corrosion resistance and biocompatibility of 316L stainless steel for biomedical applications. The microstructure and corrosion behavior are significant factors in the developmental approach in order to focus and gain promising results from 316L stainless steel. The physiological conditions throughout the body have been used to identify the potential similarities or differences to newly altered surface treatments. A complete surface characterization of all the treatments provided a stable passive oxide film for improved biocompatibility and corrosion resistance. This allowed the analytical investigation of quantitative and qualitative results to be learned and understood for the possible effects of cell response during the study.

Currently trending is the use of 316L stainless steel alloys as metallic biomaterials in orthopedic and stent implants due to their capability of yielding a biocompatible product. This idea of exploiting the possibilities of surface treated implants in compliance with necessary measures for insuring the safety of the implant should be accomplished while presenting no adverse effects regarding the physiological or biological system.

According to the data, the XPS analysis of high resolution spectras with survey, depth profile, and peak fitting scans have shown a proficient increase in a strong and stable oxide substrate to combat corrosion. The investigations of the alloying elements under etch profiling

yielded valid results, as the sputtering rate was relatively similar for that of chromium, iron, and nickel oxides compared to other researchers. This protective passive film is the foundation of many variables when considering the corrosion resistance to better the biocompatibility. The inclusions in the above oxygen evolution would indicate the relevance of oxygen removing ions at an exponential rate and thus creating abnormal inclusions compared to the smooth surfaces from the current density plateau. As the below oxygen evolution is correlated to the amount of fewer oxygen dissolution formations, hence decreased inclusions. The perpetual instigation of roughness has shown that the exchanges between surface area and contours have a dexterous effect to the corrosion imitation and cell adhesion. Thus, the cohesion relation between roughness and wettability will desirably share quality properties. The higher wettability of the surface exhibiting hydrophilic characteristics inversely has relations with the roughness surface area as the surface tension decreases. Beneficially, cell adhesion and attachment occur with these characteristics before displaying cell proliferation with the surrounding environment.

Investigating the performance of the four surface treatments considered for implant applications, the applied studies indicate good biocompatibility. However, challenges in evaluation of consistency of trials to establish the long term biocompatibility within the body should be further studied to gain additional information.

REFERENCES

[1] "Nature," *U.S National Library of Medicine*, Nov-2006.

[2] D. F. Williams, "On the nature of biomaterials," *Biomaterials*, vol. 30, no. 30, pp. 5897–5909, 2009.

[3] B. D. Ratner, *Biomaterials Science: An Introduction to Materials in Medicine*. 1996.

[4] W. Höland, M. Schweiger, R. Watzke, A. Peschke, and H. Kappert, "Ceramics as biomaterials for dental restoration.," *Expert Rev. Med. Devices*, vol. 5, no. 6, pp. 729–745, 2008.

[5] P. Parida, A. Behera, and S. C. Mishra, "Classification of Biomaterials used in Medicine," *Int. J. Adv. Appl. Sci.*, vol. 1, no. 3, pp. 125–129, 2012.

[6] N. Huebsch and D. J. Mooney, "Inspiration and application in the evolution of biomaterials.," *Nature*, vol. 462, no. 7272, pp. 426–432, 2009.

[7] J. L. Tan, J. Tien, D. M. Pirone, D. S. Gray, K. Bhadriraju, and C. S. Chen, "Cells lying on a bed of microneedles: an approach to isolate mechanical force.," *Proc. Natl. Acad. Sci. U. S. A.*, vol. 100, no. 4, pp. 1484–1489, 2003.

[8] K. T. Nam, D.-W. Kim, P. J. Yoo, C.-Y. Chiang, N. Meethong, P. T. Hammond, Y.-M. Chiang, and A. M. Belcher, "Virus-enabled synthesis and assembly of nanowires for lithium ion battery electrodes.," *Science*, vol. 312, no. 5775, pp. 885–888, 2006.

[9] W. M. Shih, J. D. Quispe, and G. F. Joyce, "A 1.7-kilobase single-stranded DNA that folds into a nanoscale octahedron.," *Nature*, vol. 427, no. 6975, pp. 618–621, 2004.

[10] T. R. Kyriakides, M. J. Foster, G. E. Keeney, A. Tsai, C. M. Giachelli, I. Clark-Lewis, B. J. Rollins, and P. Bornstein, "The CC chemokine ligand, CCL2/MCP1, participates in macrophage fusion and foreign body giant cell formation.," *Am. J. Pathol.*, vol. 165, no. 6, pp. 2157–2166, 2004.

[11] J. Black, "The education of the biomaterialist: report of a survey, 1980-81.," *J. Biomed. Mater. Res.*, vol. 16, no. 2, pp. 159–167, 1982.

[12] J. D. Bronzino, *The Biomedical Engineering Handbook*, vol. 2, no. 2. 2000.

[13] M. N. Helmus, D. F. Gibbons, and D. Cebon, "Biocompatibility: meeting a key functional requirement of next-generation medical devices.," *Toxicol. Pathol.*, vol. 36, no. 1, pp. 70–80, 2008.

[14] W. C. Billotte, *Biomaterials: Principles and Applications*. 2006.

[15] T. Tateishi, "Biomaterials in Asia: In Commemoration of the 1st Asian Biomaterials Congress," *Biomater. Asia Commem. 1st Asian Biomater. Congr.*, 2008.

[16] A. Atala, R. Lanza, J. A. Thomson, and R. M. Nerem, *Principles of Regenerative Medicine*. .

[17] Y. R. Yoo, H. H. Cho, S. G. Jang, K. Y. Lee, H. Y. Son, J. G. Kim, and Y. S. Kim, "Effect of Co Content on the Corrosion of High Performance Stainless Steels in Simulated Bio Solutions," *Key Eng. Mater.*, vol. 342–343, pp. 585–588, 2007.

[18] U. Kamachimudali, T. M. Sridhar, and B. Raj, "Corrosion of bio implants," *Sadhana*, vol. 28, no. 3–4. pp. 601–637, 2003.

[19] R. Rokicki, "Electrobright Electropolishing Service for Special Alloys and Metals including Nitinol Electropolishing, Titanium, Stainless Steel and Aluminum," *Electrobright, Electropolishing Services*. .

[20] T. Hryniewicz, R. Rokicki, and K. Rokosz., "Magnetoelectropolishing for Metal Surface Modification," *Trans. Inst. Met. Finish.*, vol. 85, pp. 325–32, 2007.

[21] J. B. Park and R. S. Lakes, *Biomaterials, an Introduction*. 2007.

[22] A. D. Mazzocca, J. P. DeAngelis, A. E. Caputo, B. D. Browner, J. W. Mast, and M. W. Mendes, *Principles of Internal Fixation, in: B.D. Browner (Ed.), Skeletal Trauma*. Philadelphia: W.B. Saunders Company, 2008.

[23] D. J. Blackwood, "Biomaterials: Past Successes and Future Problems," *Corrosion Reviews*, vol. 21, no. 2–3. 2003.

[24] Q. Chen and G. Thouas, *Biomaterials: A Basic Introduction*. Boca Raton, FL: Taylor & Francis Group, 2014.

[25] A. F. Recum and S. Strauss, *Handbook of Biomaterials Evaluation: Scientific, Technical and Clinical Testing of Implant Materials*. Philadelphia, USA: Taylor & Francis, 1998.

[26] D. F. Williams, "Definitions in biomaterials: proceedings of a consensus conference of the European Society for Biomaterials," 1987.

[27] J. Black, G. W. Hastings, and D. F. Williams, *General Concepts of Biocompatibilitty, in: J. Black, G.W. Hastings (Eds.), Handbook of Biomaterials Properties.* New York: Chapman and Hall, 1998.

[28] R. Yoda, "Elastomers for biomedical applications.," *J. Biomater. Sci. Polym. Ed.*, vol. 9, no. 6, pp. 561–626, 1998.

[29] P. Vermette, H. J. Griesser, G. Laroche, Y. Marois, and R. Guidoin, *Biocompatibility of Polyurethanes, in: P. Vermette, H.J. Griesser, G. Laroche, R. Guidoin (Eds.), Biomedcial Applications of Polyurethanes*. Georgetown, TX: Landies Bioscience, 2001.

[30] J. J. Jacobs, A. K. Skipor, L. M. Patterson, N. J. Hallab, W. G. Paprosky, J. Black, and J. O. Galante, "Metal release in patients who have had a primary total hip arthroplasty. A prospective, controlled, longitudinal study," *J Bone Jt. Surg Am*, vol. 80, no. 10, pp. 1447–1458, 1998.

[31] J. J. Jacobs, C. Silverton, N. J. Hallab, A. K. Skipor, L. Patterson, J. Black, and J. O. Galante, "Metal release and excretion from cementless titanium alloy total knee replacements.," *Clin. Orthop. Relat. Res.*, no. 358, pp. 173–180, 1999.

[32] M. Sumita, T. Hanawa, I. Ohnishi, and T. Yoneyama, "Failure Processes in Biometallic Materials," *Compr. Struct. Integr.*, vol. 9, pp. 131–167, 2003.

[33] M. Long and H. J. Rack, "Titanium alloys in total joint replacement--a materials science perspective.," *Biomaterials*, vol. 19, no. 18, pp. 1621–1639, 1998.

[34] R. R. Seeley, T. D. Stephens, and P. Rate, *Anatomy and Physiology*. New York: McGrew Hill, 2006.

[35] E. Whitney and S. R. Rolfes, *Understanding Nutrition*. 2012.

[36] D. G. Barceloux, "Cobalt.," *J. Toxicol. Clin. Toxicol.*, vol. 37, no. 2, pp. 201–216, 1999.

[37] M. B. Nasab, M. R. Hassan, and B. Bin Sahari, "Metallic biomaterials of knee and hip - A review," *Trends in Biomaterials and Artificial Organs*, vol. 24, no. 2. pp. 69–82, 2010.

[38] A. Parsapour, M. H. Fathi, M. Salehi, A. Saatchi, and M. Mehdikhani, "The Effect of Surface Treatment on Corrosion behavior of Surgical 316L Stainless Steel Implant," *Int. J. Iron Steel Soc. Iran*, vol. 28, no. 2, pp. 125–131, 2007.

[39] R. L. Sammons, *Modifying Biomaterial Surfaces to Optimise Interactions with Bone, in: R. Williams (Ed.), Surface Modification of Biomaterials; Methods, Analysis and Applications*. Oxford: Woodhead Publishing, 2011.

[40] A. Yamamoto, R. Honma, and M. Sumita, “Cytotoxicity evaluation of 43 metal salts using murine fibroblasts and osteoblastic cells,” *J. Biomed. Mater. Res.*, vol. 39, no. 2, pp. 331–340, 1998.

[41] J. R. Davis, *Handbook of Materials for Medical Devices*. 2003.

[42] J. Alvarado, R. Maldonado, J. Marxuach, and R. Otero, “Biomechanics of Hip and Knee Prostheses: Applications of Engineering Mechanics in Medicine,” *Appl. Eng. Mech. Med.*, no. December, pp. 6–22, 2003.

[43] M. Navarro, A. Michiardi, O. Castaño, and J. A. Planell, “Biomaterials in orthopaedics.,” *J. R. Soc. Interface*, vol. 5, no. 27, pp. 1137–1158, 2008.

[44] Q. Doran, F. C. Law, M. J. Allen, and N. Rushton, “Neoplastic Transformation of Cells by Soluble but not Particulate Forms of Metals Used in Orthopaedic Implants,” *Biomaterials*, vol. 19, no. 7–9, pp. 751–759, 1998.

[45] K. Cheney, C. Gumbiner, B. Benson, and M. Tenenbein, *Survival after a severe iron poisoning treated with intermittent infusions of deferoxamine.*, vol. 33, no. 1. 1995, pp. 61–66.

[46] A. B. Abdel-Mageed and F. W. Oehme, “A Review of the Biochemical Roles, Toxicity and Interactions of Zinc, Copper and Iron: I. Zinc.,” *Vet. Hum. Toxicol.*, vol. 32, no. 1, pp. 34–39, 1990.

[47] C. Esteve, E. Alcaide, and R. Ureña, “The Effect of Metals on Condition and Pathologies of European Eel (Anguilla Anguilla): In Situ and Laboratory Experiments,” *Aquat. Toxicol.*, vol. 109, pp. 176–184, 2012.

[48] A. D. Dayan and A. J. Paine, “Mechanisms of chromium toxicity, carcinogenicity and allergenicity: review of the literature from 1985 to 2000.,” *Hum. Exp. Toxicol.*, vol. 20, no. 9, pp. 439–451, 2001.

[49] D. G. Barceloux, “Chromium.,” *J. Toxicol. Clin. Toxicol.*, vol. 37, no. 2, pp. 173–194, 1999.

[50] D. M. Stearns and K. E. Wetterhahn, “Abstracts of Papers of the American Chemical Society,” *Am. Chem. Soc.*, vol. 212, 1996.

[51] D. Colomb, H. Perrot, and A. J. Beyvin, “Ulcers in a person working with chromium,” *Bull. Soc. Fr. Dermatol. Syphiligr*, vol. 76, pp. 130–131, 1969.

[52] S. Burkhardt, R. J. Reiter, D. X. Tan, R. Hardeland, J. Cabrera, and M. Karbownik, “DNA oxidatively damaged by chromium(III) and H2O2 is protected by the antioxidants melatonin, N1-acetyl-N2-formyl-5-methoxykynuramine, resveratrol and uric acid,” *Int. J. Biochem. Cell Biol.*, vol. 33, no. 8, pp. 775–783, 2001.

[53] E. Rudolf and M. Cervinka, “Trivalent chromium activates Rac-1 and Src and induces switch in the cell death mode in human dermal fibroblasts,” *Toxicol. Lett.*, vol. 188, no. 3, pp. 236–242, 2009.

[54] K. Hughes, M. E. Meek, P. K. L. Chan, J. Shedden, S. Bartlett, and L. J. Seed, “Nickel and its Compounds: Evaluation of Risks to Health from Environmental Exposure in Canada,” 1994.

[55] R. B. Ashman, J. G. Birch, L. B. Bone, J. D. Corin, J. A. Herring, C. E. Johnston, J. F. Ritterbush, and J. W. Roach, “Mechanical testing of spinal instrumentation.,” *Clin. Orthop. Relat. Res.*, vol. 227, pp. 113–125, 1988.

[56] J. Zhao, X. Shi, V. Castranova, and M. Ding, “Occupational toxicology of nickel and nickel compounds.,” *J. Environ. Pathol. Toxicol. Oncol.*, vol. 28, no. 3, pp. 177–208, 2009.

[57] F. W. Sunderman, “Physicochemical and biological attributes of nickel compounds in relationship to carcinogenic activities,” *J. UOEH*, vol. 9, no. SUPPL., pp. 84–94, 1987.

[58] Q. Chen and G. A. Thouas, “Metallic implant biomaterials,” *Mater. Sci. Eng. R Reports*, vol. 87, pp. 1–57, 2015.

[59] C. B. Klein, K. Conway, X. W. Wang, R. K. Bhamra, X. H. Lin, M. D. Cohen, L. Annab, J. C. Barrett, and M. Costa, “Senescence of nickel-transformed cells by an X chromosome: possible epigenetic control.,” *Science*, vol. 251, no. 4995, pp. 796–799, 1991.

[60] A. Madhan Kumar and N. Rajendran, “Electrochemical aspects and in vitro biocompatibility of polypyrrole/TiO2 ceramic nanocomposite coatings on 316L SS for orthopedic implants,” *Ceram. Int.*, vol. 39, no. 5, pp. 5639–5650, 2013.

[61] C. Liu, G. Lin, D. Yang, and M. Qi, “In vitro corrosion behavior of multilayered Ti/TiN coating on biomedical AISI 316L stainless steel,” *Surf. Coatings Technol.*, vol. 200, no. 12–13, pp. 4011–4016, 2006.

[62] K. Y. Chiu, F. T. Cheng, and H. C. Man, “Corrosion behavior of AISI 316L stainless steel surface-modified with NiTi,” *Surf. Coatings Technol.*, vol. 200, no. 20–21, pp. 6054–6061, 2006.

[63] G. Mani, M. D. Feldman, D. Patel, and C. M. Agrawal, “Coronary Stents: A Materials Perspective,” *Biomaterials*, vol. 28, no. 9. pp. 1689–1710, 2007.

[64] T. Hryniewicz, R. Rokicki, and K. Rokosz, “Surface Characterization of AISI 316L Biomaterials Obtained by Electropolishing in a Magnetic Field,” *Surf. Coatings Technol.*, vol. 202, pp. 1668–1673, 2008.

[65] B. Liu and Y. F. Zheng, “Effects of alloying elements (Mn, Co, Al, W, Sn, B, C and S) on biodegradability and in vitro biocompatibility of pure iron.,” *Acta Biomater.*, vol. 252, no. February, pp. 151–156, 2010.

[66] D. Gopi, D. Rajeswari, S. Ramya, M. Sekar, R. Pramod, J. Dwivedi, L. Kavitha, and R. Ramaseshan, “Enhanced corrosion resistance of strontium hydroxyapatite coating on electron beam treated surgical grade stainless steel,” *Appl. Surf. Sci.*, vol. 286, pp. 83–90, 2013.

[67] M. K. Lei and X. M. Zhu, “In vitro corrosion resistance of plasma source ion nitrided austenitic stainless steels,” *Biomaterials*, vol. 22, no. 7, pp. 641–647, 2001.

[68] A. Latifi, M. Imani, M. T. Khorasani, and M. D. Joupari, “Electrochemical and chemical methods for improving surface characteristics of 316L stainless steel for biomedical applications,” *Surf. Coatings Technol.*, vol. 221, pp. 1–12, 2013.

[69] M. Haïdopoulos, S. Turgeon, C. Sarra-Bournet, G. Laroche, and D. Mantovani, “Development of an optimized electrochemical process for subsequent coating of 316 stainless steel for stent applications,” *J. Mater. Sci. Mater. Med.*, vol. 17, no. 7, pp. 647–657, 2006.

[70] W. Zhou, X. Zhong, X. Wu, L. Yuan, Z. Zhao, H. Wang, Y. Xia, Y. Feng, J. He, and W. Chen, “The effect of surface roughness and wettability of nanostructured TiO2 film on TCA-8113 epithelial-like cells,” *Surf. Coatings Technol.*, vol. 200, no. 20–21, pp. 6155–6160, 2006.

[71] C. C. Shih, C. M. Shih, Y. Y. Su, L. H. J. Su, M. S. Chang, and S. J. Lin, “Effect of surface oxide properties on corrosion resistance of 316L stainless steel for biomedical applications,” *Corros. Sci.*, vol. 46, no. 2, pp. 427–441, 2004.

[72] M. Haïdopoulos, S. Turgeon, G. Laroche, and D. Mantovani, “Chemical and morphological characterization of ultra-thin fluorocarbon plasma-polymer deposition on 316 stainless steel substrates: A first step toward the improvement of the long-term safety of coated-stents,” *Plasma Process. Polym.*, vol. 2, no. 5, pp. 424–440, 2005.

[73] I. D. Scheerder, J. Sohier, K. A. I. Wang, E. Verbeken, X. R. Zhou, L. Froyen, J. A. N. Van Humbeeck, J. A. N. Piessens, and F. Van De Werf, “Metallic Surface Treatment Using Electrochemical Polishing Decreases Thrombogenicity and Neointimal Hyperplasia of Coronary Stents,” *J. Interv. Cardiol.*, vol. 13, no. 3, pp. 179–185, 2000.

[74] E. J. Sutow, “The influence of electropolishing on the corrosion resistance of 316L stainless steel.,” *J. Biomed. Mater. Res.*, vol. 14, no. 5, pp. 587–595, 1980.

[75] G. Beilby, *Aggregation and Flow of Solids*. London, Macmillan and co., limited, 1921.

[76] T. P. Hoar, D. C. Mears, and G. P. Rothwell, "The relationships between anodic passivity, brightening and pitting," *Corrosion Science*, vol. 5, no. 4. pp. 279–289, 1965.

[77] R. Rokicki and T. Hryniewicz, "Enhanced Oxidation-Dissolution Theory of Electropolishing," *Trans. Inst. Met. Finish.*, vol. 90, no. 4, pp. 188–196, 2012.

[78] R. Rokicki, "Magnetic Fields and Electropolished Metallic Implants," *Medical Device*, vol. 28. pp. 116–123, 2006.

[79] T. Hryniewicz, S. J. Fernandes, and R. Rokicki, "Comparative Auger Studies of 316L Stainless Steel," 2006.

[80] T. Hryniewicz and R. Rokicki, "On the Surface Modification of Stainless Steels, in: David Hui (Ed.), Proc. of 15th Annual Intl. Confer. on Composites/Nano-Engineering," pp. 345–346, 2007.

[81] T. Hryniewicz, R. Rokicki, and K. Rokosz, "Modification of Stainless Steel Surface by Magnetoelectropolishing," *Proc. 5th Sci. Confer. Mech.*, no. 1–8, 2007.

[82] T. Hryniewicz, K. Rokosz, and R. Rokicki, "Electrochemical and XPS Studies of AISI 316L Stainless Steel After Electropolishing in a Magnetic Field," *Corros. Sci.*, vol. 50, no. 9, pp. 2676–2681, 2008.

[83] T. Hryniewicz, K. Rokosz, and R. Rokicki, "Magnetoelectropolishing Process Improves Characteristics of Finished Metal Surfaces," *Met. Finish.*, vol. 104, no. 12, pp. 26–33, 2006.

[84] ASM International Handbook, *Properties and Selection: Irons, Steels, and High-Performance Alloys*, vol. 1. Materials Park, OH: ASM International, 1990.

[85] P. Dettner, *Electrolytic and Chemical Polishing of Metals*. Ordentlich Publishers, 1987.

[86] T. Hryniewicz and K. Rokosz, "Analysis of XPS results of AISI 316L SS electropolished and magnetoelectropolished at varying conditions," *Surf. Coatings Technol.*, vol. 204, no. 16–17, pp. 2583–2592, 2010.

[87] T. Hryniewicz and K. Rokosz, "Investigation of selected surface properties of AISI 316L SS after magnetoelectropolishing," *Mater. Chem. Phys.*, vol. 123, no. 1, pp. 47–55, 2010.

[88] H. M. Burt and W. L. Hunter, "Drug-Eluting Stents: An Innovative Multidisciplinary Drug Delivery Platform," *Advanced Drug Delivery Reviews*, vol. 58. pp. 345–356, 2006.

[89] G. J. Adams, U. Baltazar, C. Karmonik, C. Bordelon, P. H. Lin, R. L. Bush, A. B. Lumsden, and J. D. Morrisett, "Comparison of 15 Different Stents in Superficial Femoral Arteries by High Resolution MRI Ex Vivo and In-Vivo," *J. Magn. Reson. Imaging*, vol. 22, no. 1, pp. 125–135, 2005.

[90] H. M. Krumholz, E. D. Peterson, J. Z. Ayanian, M. H. Chin, R. F. DeBusk, L. Goldman, C. I. Kiefe, N. R. Powe, J. S. Rumsfeld, J. A. Spertus, and W. S. Weintraub, "Report of the National Heart, Lung, and Blood Institute working group on outcomes research in cardiovascular disease," *Circulation*, vol. 111, no. 23, pp. 3158–3166, 2005.

[91] J. Bogaert, S. Dymarkowski, and A. Taylor, "Coronary Artery Disease, in: J. Bogaert, S. Dymarkowski, A. Taylor (Eds.)," *Clin. Card. MRI*, pp. 381–437, 2005.

[92] H. W. Roberts and S. W. Redding, "Coronary artery stents: review and patient-management recommendations.," *J. Am. Dent. Assoc.*, vol. 131, no. 6, pp. 797–801, 2000.

[93] H. S. Lett, "Depression as a Risk Factor for Coronary Artery Disease: Evidence, Mechanisms, and Treatment," *Psychosomatic Medicine*, vol. 66, no. 3. pp. 305–315, 2004.

[94] S. Windecker, R. Simon, M. Lins, V. Klauss, F. R. Eberli, M. Roffi, G. Pedrazzini, T. Moccetti, P. Wenaweser, M. Togni, D. Tüller, R. Zbinden, C. Seiler, J. Mehilli, A. Kastrati, B. Meier, and O. M. Hess, "Randomized comparison of a titanium-nitride-oxide-coated stent with a stainless steel stent for coronary revascularization - The TiNOX trial," *Circulation*, vol. 111, no. 20, pp. 2617–2622, 2005.

[95] J. Pan, C. Karlén, and C. Ulfvin, "Electrochemical study of resistance to localized corrosion of stainless steels for biomaterial applications," *J. Electrochem. Soc.*, vol. 147, no. 3, pp. 1021–1025, 2000.

[96] U. Baber, R. Mehran, S. K. Sharma, S. Brar, J. Yu, J. W. Suh, H. S. Kim, S. J. Park, A. Kastrati, A. De Waha, P. Krishnan, P. Moreno, J. Sweeny, M. C. Kim, J. Suleman, R. Pyo, J. Wiley, J. Kovacic, A. S. Kini, and G. D. Dangas, "Impact of the everolimus-eluting stent on stent thrombosis: A meta-analysis of 13 randomized trials," *J. Am. Coll. Cardiol.*, vol. 58, no. 15, pp. 1569–1577, 2011.

[97] C. C. Shih, C. M. Shih, Y. Y. Su, L. H. J. Su, M. S. Chang, and S. J. Lin, "Quantitative evaluation of thrombosis by electrochemical methodology," *Thromb. Res.*, vol. 111, no. 1–2, pp. 103–109, 2003.

[98] K. C. Dee, D. A. Puleo, and R. Bizios, *An Introduction to Tissue-Biomaterial Interactions*. Hoboken, NJ: John Wiley & Sons Inc., 2003.

[99] X. Wang, X. Zhang, J. Castellot, I. Herman, M. Iafrati, and D. L. Kaplan, "Controlled release from multilayer silk biomaterial coatings to modulate vascular cell responses," *Biomaterials*, vol. 29, no. 7, pp. 894–903, 2008.

[100] R. V. Stan, "In-Vitro Vascular Cell Culture Systems – Endothelial Cell Culture Systems," in *Comprehensive Toxicology*, Elsevier, Oxford, 2010, pp. 97–111.

[101] C. Mrowietz, R. P. Franke, U. T. Seyfert, J. W. Park, and F. Jung, "Haemocompatibility of polymer-coated stainless steel stents as compared to uncoated stents.," *Clin. Hemorheol. Microcirc.*, vol. 32, no. 2, pp. 89–103, 2005.

[102] E. Mihalyi, "Transformation of Fibrinogen into Fibrin. I. Electrochemical Investigation of the Activation Process.," *J. Biol. Chem.*, vol. 209, pp. 723–32, 1954.

[103] S. A. Biela, Y. Su, J. P. Spatz, and R. Kemkemer, "Different sensitivity of human endothelial cells, smooth muscle cells and fibroblasts to topography in the nano-micro range," *Acta Biomater*, vol. 5, pp. 2460–2466, 2009.

[104] B. P. Yan, S. J. Duffy, D. J. Clark, J. Lefkovits, R. Warren, R. Gurvitch, R. Lew, M. Sebastian, A. Brennan, N. Andrianopoulos, C. M. Reid, and A. E. Ajani, "Rates of Stent Thrombosis in Bare-Metal Versus Drug-Eluting Stents (from a Large Australian Multicenter Registry)," *Am. J. Cardiol.*, vol. 101, no. 12, pp. 1716–1722, 2008.

[105] F. J. Jing, N. Huang, L. Wang, R. K. Y. Fu, Y. F. Mei, Y. X. Leng, J. Y. Chen, X. Y. Liu, and P. K. Chu, "Behavior of Human Umbilical Vein Endothelial Cells on Micro-Patterned Amorphous Hydrogenated Carbon Films Produced by Plasma Immersion Ion Implantation & Deposition and Plasma tching," *Diam. Relat. Mater.*, vol. 16, no. 3, pp. 550–557, 2007.

[106] T. W. Chung, D. Z. Liu, S. Y. Wang, and S. S. Wang, "Enhancement of the growth of human endothelial cells by surface roughness at nanometer scale," *Biomaterials*, vol. 24, no. 25, pp. 4655–4661, 2003.

[107] M. N. Babapulle and M. J. Eisenberg, "Coated Stents for the Prevention of Restenosis: Part I," pp. 2734–2740, 2002.

[108] Z. Shi, Y. Wang, C. Du, N. Huang, L. Wang, and C. Ning, "Silicon nitride films for the protective functional coating: Blood compatibility and biomechanical property study," *Journal of the Mechanical Behavior of Biomedical Materials*. 2012.

[109] S. Habibzadeh, L. Li, S. Omanovic, D. Shum-Tim, and E. C. Davis, "Biocompatibility of Ir/Ti-oxide coatings: Interaction with platelets, endothelial and smooth muscle cells," *Appl. Surf. Sci.*, vol. 301, pp. 530–538, 2014.

[110] E. Alt and L. J. Stotts, "Vascular and Endoluminal Stents with Iridium Oxide Coating," 1999.

[111] S. Habibzadeh, D. Shum-tim, and S. Omanovic, "Surface and Electrochemical Characterization of IrTi-Oxide Coatings: Towards the Improvement of Radiopacity for Coronary Stent Applications," vol. 8, pp. 6291–6310, 2013.

[112] F. Rupp, L. Scheideier, N. Olshanska, M. De Wild, M. Wieland, and J. Geis-Gerstorfer, "Enhancing surface free energy and hydrophilicity through chemical modification of

microstructured titanium implant surfaces," *J. Biomed. Mater. Res. - Part A*, vol. 76, no. 2, pp. 323–334, 2006.

[113] P. I. Brånemark, "Osseointegration and its experimental background.," *J. Prosthet. Dent.*, vol. 50, no. 3, pp. 399–410, 1983.

[114] J. E. Feighan, V. M. Goldberg, D. Davy, J. A. Parr, and S. Stevenson, "The influence of surface-blasting on the incorporation of titanium-alloy implants in a rabbit intramedullary model.," *J. Bone Joint Surg. Am.*, vol. 77, no. 9, pp. 1380–1395, 1995.

[115] R. B. Alvarez, H. J. Martin, M. F. Horstemeyer, M. Q. Chandler, N. Williams, P. T. Wang, and A. Ruiz, "Corrosion relationships as a function of time and surface roughness on a structural AE44 magnesium alloy," *Corros. Sci.*, vol. 52, no. 5, pp. 1635–1648, 2010.

[116] K. Kieswetter, Z. Schwartz, T. W. Hummert, D. L. Cochran, J. Simpson, D. D. Dean, and B. D. Boyan, "Surface roughness modulates the local production of growth factors and cytokines by osteoblast-like MG-63 cells," *J. Biomed. Mater. Res.*, vol. 32, no. 1, pp. 55–63, 1996.

[117] X. Zhu, J. Chen, L. Scheideler, R. Reichl, and J. Geis-Gerstorfer, "Effects of topography and composition of titanium surface oxides on osteoblast responses," *Biomaterials*, vol. 25, no. 18, pp. 4087–4103, 2004.

[118] K. Kyobum, "Scaffold Design Parameters to Stimulate the Osteogenic Signal for Bone Tissure Engineering Applications," University of Maryland, 2010.

[119] S. L. Rose and J. E. Babensee, "Complimentary endothelial cell/smooth muscle cell Co-culture systems with alternate smooth muscle cell phenotypes," *Ann. Biomed. Eng.*, vol. 35, no. 8, pp. 1382–1390, 2007.

[120] A. Shahryari, F. Azari, H. Vali, and S. Omanovic, "The response of fibrinogen, platelets, endothelial and smooth muscle cells to an electrochemically modified SS316LS surface: Towards the enhanced biocompatibility of coronary stents," *Acta Biomater.*, vol. 6, no. 2, pp. 695–701, 2010.

APPENDIX

BIOGRAPHICAL SKETCH

Lawrence Cano earned his Bachelor of Science in Mechanical Engineering in the Fall of 2011 at the University of Texas – Pan American. Immediately following graduation, he was offered a position with Halliburton field services as a fracture engineer where he studied and learned the concepts of fracturing shale formations for efficient oil and gas extraction. Some time after, he was accepted into graduate school at the University of Texas – Pan American in hopes of pursuing a Master of Science degree in Mechanical Engineering and specializing in Material Science. During his Master's studies, his was offered an internship with the General Electric Aviation Company (GE Aviation) to work fulltime where he undertook a production and product engineer role in his one year contract while attending evening lectures. After completion of his internship, Lawrence decided and began the process on his graduate research studies for surface characterizing 316L stainless steel. He received his Master of Science in Mechanical Engineering from the University of Texas – Pan American in May 2015.

Mailing Address: 2319 Liberty Street, Mercedes, TX 78570